Check for updates

Mucosa-interfacing electronics

Kewang Nan[1,2,4], Vivian R. Feig[2,3,4], Binbin Ying[1,2,4], Julia G. Howarth[1], Ziliang Kang[1,2], Yiyuan Yang[1] and Giovanni Traverso[1,2] ✉

Abstract | The surface mucosa that lines many of our organs houses myriad biometric signals and, therefore, has great potential as a sensor–tissue interface for high-fidelity and long-term biosensing. However, progress is still nascent for mucosa-interfacing electronics owing to challenges with establishing robust sensor–tissue interfaces; device localization, retention and removal; and power and data transfer. This is in sharp contrast to the rapidly advancing field of skin-interfacing electronics, which are replacing traditional hospital visits with minimally invasive, real-time, continuous and untethered biosensing. This Review aims to bridge the gap between skin-interfacing electronics and mucosa-interfacing electronics systems through a comparison of the properties and functions of the skin and internal mucosal surfaces. The major physiological signals accessible through mucosa-lined organs are surveyed and design considerations for the next generation of mucosa-interfacing electronics are outlined based on state-of-the-art developments in bio-integrated electronics. With this Review, we aim to inspire hardware solutions that can serve as a foundation for developing personalized biosensing from the mucosa, a relatively uncharted field with great scientific and clinical potential.

The traditional paradigm for medical diagnostics, which is still actively practised around the globe, relies on physicians' use of their five basic senses to make inferences about a patient's health[1]. For example, palpation through orifices such as the oral cavity, rectum or vaginal canal is still the predominant diagnostic mechanism within the digestive and female reproductive tracts[2]. Although inexpensive and straightforward, such subjective methods are prone to error and bias[2]. A growing trend is to replace physicians' own senses with electronic sensors, which not only enhances the range and quality of detection but also provides a means of establishing 'ground truths' for pathological conditions based on the collection of large clinically acquired datasets[3]. For example, touch can be replaced with tactile, pressure and strain sensors; hearing with acoustic and ultrasonic sensors; and smell and taste with biochemical sensors, all of which provide objective measurements. As traditional sensing instruments have evolved from bulky and tethered systems into portable and miniaturized electronics that can be worn continuously away from the clinic, digital diagnostics have transformed from being scattered and requiring restriction in movement to mitigate compromise of sensor–tissue interfacing to becoming continuous and unconfined, reducing patient burden while improving health outcomes by enabling earlier and faster detection[4].

Establishing minimally invasive, high-fidelity and long-term sensing interfaces with the human body has been the primary driving force for skin-interfacing electronics (SIE), a class of technologies initially developed for prosthetic control systems[5] that has since made remarkable advances towards the introduction of personalized health-care approaches (FIG. 1). SIE refers to electronics that seamlessly interact with skin owing to their physical properties, which closely match those of skin, including flexibility and stretchability[6]. Major hardware breakthroughs over the past decade, including the development of soft sensors, wireless technologies and battery-free powering solutions, have enabled SIE to provide minimally invasive, real-time, continuous and untethered health monitoring[4,7]. The engineering and applications of SIE are reviewed elsewhere[8–11].

Despite these advances, myriad relevant physiological and pathophysiological signals are inaccessible from the skin, including those from the digestive, respiratory, reproductive and urinary systems. These anatomical regions are covered by mucosa, which is often referred to as the 'inner skin' of the body and has many anatomical and functional similarities with skin[12]. Existing clinically approved sensors that interact with the mucosa (FIG. 1) in a minimally invasive way are in capsule or catheter forms; rigid or with limited bendability; battery-powered or tethered; are incapable of being retained by the body for long-term measurements; and have more technical similarities with conventional electronics than with SIE[13]. These design features are insufficient to achieve comprehensive monitoring of the mucosa, or organs underlying the mucosa, in a tissue-interfacing and chronic fashion. In this Review, we explore how many

[1]*Department of Mechanical Engineering, Massachusetts Institute of Technology, Cambridge, MA, USA.*

[2]*Division of Gastroenterology, Hepatology and Endoscopy, Brigham and Women's Hospital, Harvard Medical School, Boston, MA, USA.*

[3]*Koch Institute for Integrative Cancer Research, Massachusetts Institute of Technology, Cambridge, MA, USA.*

[4]*These authors contributed equally: Kewang Nan, Vivian R. Feig, Binbin Ying.*

✉*e-mail: cgt20@mit.edu*

https://doi.org/10.1038/s41578-022-00477-2

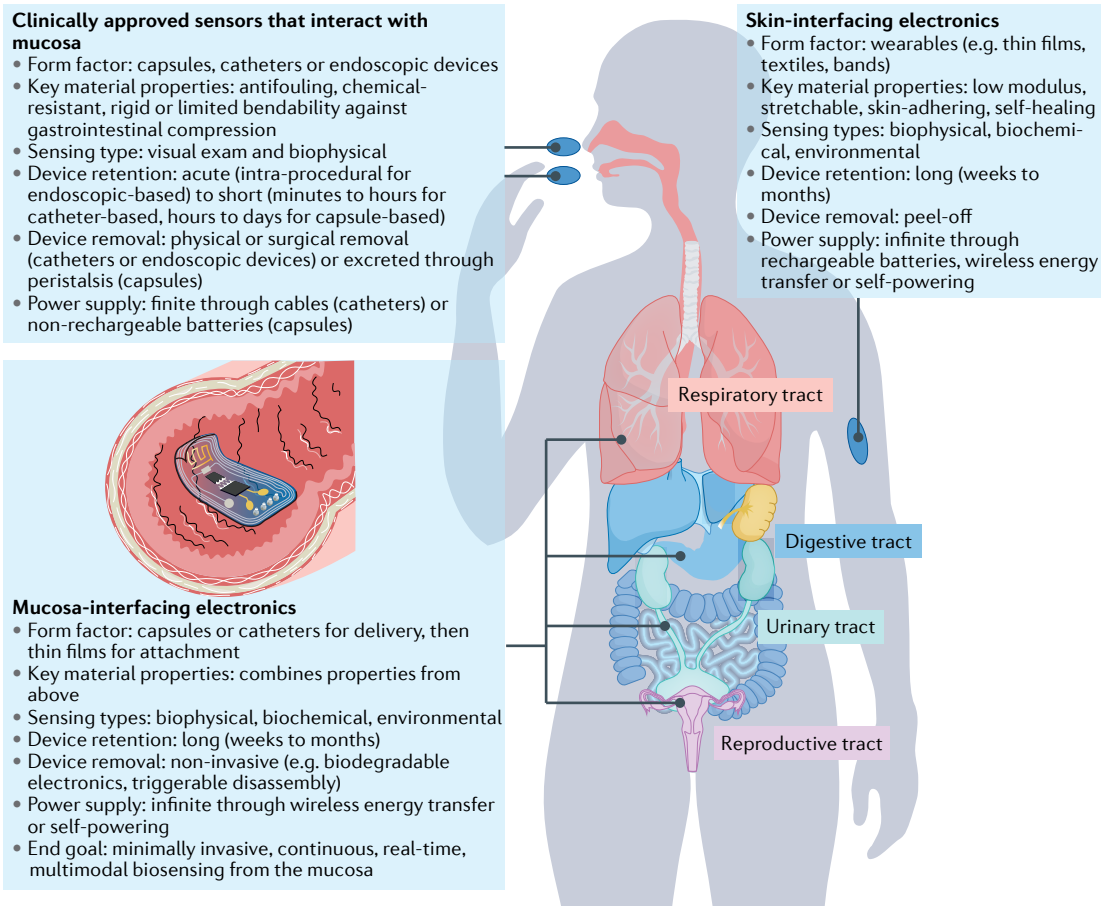

Fig. 1 | **Overview of mucosa-interfacing electronics in relation to existing sensors that interact with mucosa and the skin-interfacing electronics.** The key features of existing clinically approved sensors that interact with the mucosa and skin-interfacing electronics are highlighted, as well as the end goal for mucosa-interfacing electronics.

of the design considerations that may inform the development of truly mucosa-interfacing electronics (MIE) can be addressed by lessons learnt from SIE (FIG. 1).

This Review aims to provide guidelines to inform the design of MIE based on considerations specific to the mucosa-lined regions of the body. First, we describe the main anatomical and functional features of the mucosa and compare its properties with those of the skin (BOX 1). Next, we identify major types of physiological signals that can be accessed from the mucosa and describe how these are currently evaluated clinically. Finally, we discuss the major engineering challenges for realizing MIE and highlight how researchers have addressed these challenges through technical advances in SIE and other forms of bio-integrated electronics.

Diagnostic attributes of surface mucosa

A diverse set of sensor technologies has been exploited in SIE to measure multiple types of physiological signals from the skin: electrical, biochemical, temperature, vascular dynamics, mechanical, skin properties and environmental[8,11]. Most of these signal types are present on the mucosa with richer details and diagnostic potential (TABLE 1). In this section, we survey these accessible signal types from the mucosa and discuss existing clinical tools for accessing these signals. We note, however, that none of these methods offers minimally invasive and continuous sensing in unrestrained patients. This type of sensing is needed to enable the use of the acquired signals to obtain real-time feedback for health tracking and therapeutic interventions, as has been the trend for SIE.

Electrical signals

Electrical signals through the mucosa can be valuable indicators of health status. For instance, measuring changes in vaginal mucus impedance and uterine contractile electrical activity in pregnant women can be used to predict delivery time and identify abnormal labour conditions[14]. Similarly, pulmonary mucosal impedance directly reflects pulmonary function and can be used to monitor diseases such as pneumonia and asthma[15]. The slow-wave potential, a rhythmic electrophysiological event in the gastrointestinal (GI) tract, is highly correlated to gastric functions[16,17]. Last, the external urethral sphincter muscle regulates the timely passage of urine through the urethra, and external urethral sphincter electromyographic activity is used to study lower urinary tract function[18].

Currently, several clinical techniques are available to monitor electrical signals. A cutaneous electrogastrogram obtained from the abdominal wall, although

indirect, is used clinically to detect gastric slow-wave motility by recording myoelectrical activity[19]. Similarly, measurements of urine electromyographic activity use small sensors placed near the urethra or rectum to record muscle and nerve activity. The Digitrapper reflux testing system, a commercial product from Medtronic, can quantify acid reflux symptoms with catheter-based impedance testing[20]. In the reproductive tract, the medical-grade kegg fertility tracker device helps to more accurately predict a woman's fertile window by measuring electrolyte levels through cervical fluid impedance[21].

A major limitation of these diagnostic techniques is that they are mainly accessible only by referral through trained practitioners and often necessitate uncomfortable pre-procedure preparations. Additionally, cutaneous signal acquisition methods usually produce low signals and exhibit motion artefacts, while clinical methods that interface with the inner mucosa directly lack the possibility for long-term monitoring because they require bulky external instrumentation.

Biochemical signals

An enormous amount of biochemical information can be obtained from mucosa and the lumen of tubular organs. For example, a decrease in the oesophageal pH to <7 suggests gastro-oesophageal reflux disease[22]. Balanced electrolytes, metabolites, gas, enzymes and microorganisms in the GI tract are important for overall physical and psychological health beyond healthy GI function. The microbiome influences immune system development and function[23]. Aberrant intestinal microbiota can contribute to the pathogenesis of various metabolic disorders, including obesity, type 2 diabetes, cardio-metabolic diseases and malnutrition[24]. Additionally, DNA information from the respiratory system can help diagnose viral infections, such as SARS-CoV-2. DNA, RNA and protein

Box 1 | **The surface mucosa**

The surface mucosa is the membrane layer that lines the internal cavities and covers the surface of many organs within the digestive, urinary, female reproductive and respiratory tracts. Its outermost layer comprises a cellular epithelium akin to that which covers the skin[12]. Although there are many similarities between these epithelia, structural differences between mucosa and skin reflect their different properties and functions. Below, we highlight the key differences that inform the unique considerations for developing mucosa-interfacing systems (see Supplementary Tables 1 and 2 for further comparison).

Structure and dynamics

The outer layer of the skin is a keratinized stratified squamous epithelium that is slowly but continuously regenerated, turning over approximately once every 40–56 days (REF.[232]). The turnover rate of mucosa, by contrast, varies from complete turnover every 2–6 days in the small intestine[233] to once every 200 days in the bladder[234]. In the female reproductive system, the uterine mucosa undergoes cyclic morphological changes and turnover with hormonal fluctuations throughout the menstrual cycle, culminating in the complete shedding of the outermost layer during menstruation[235].

Mucosal surfaces are more curvilinear and dynamic than skin. For example, the digestive mucosa has a large surface area to facilitate nutrient absorption, with a highly folded structure and villi in the small intestine[236]. Muscular activity transits food down the digestive tract through peristalsis, imparting large strain[236]. Additionally, the bladder epithelium changes from cuboidal to squamous to accommodate stretching as the bladder fills and empties[237]. Finally, lung bronchi are lined with hair-like projections called cilia that beat in synchronicity to transport mucus[238].

Skin is covered by a keratinous protective layer known as the stratum corneum. By contrast, mucosal linings are generally covered by a layer of mucus — a viscoelastic mucin hydrogel primarily comprised of glycoproteins secreted by cells in the epithelium[239] — that protects the underlying cells from chemicals, enzymes, microorganisms and mechanical damage[239]. Mucus thickness ranges from 10 μm to 15 μm in the respiratory tract to 300 μm and 700 μm in the stomach and intestine, respectively[239]. In the uterus, mucus thickness and viscoelasticity vary during the menstrual cycle; for instance, cervical mucus is more watery during ovulation to facilitate sperm entry[240]. Generally, the mucus barrier is more dynamic than the underlying epithelium. In the gastrointestinal (GI) system, mucus has a turnover rate that ranges from minutes to hours[241]. The respiratory mucus interacts with cilia in a process called mucociliary clearance to trap foreign debris, which is transported with the mucus out of the airways by ciliary beating[238].

Chemical and biological environments

Mucosal surroundings are often more chemically and biologically extreme than those of skin. Mucosal surfaces typically experience higher hydration levels than skin, particularly in the GI tract, where up to 9 l of fluid is transported daily[242]. The GI tract also contains a diverse set of endogenous and dietary proteins that have roles in digestive processes[243]. In the urinary tract, chemicals such as uric acid and calcium oxalate can form into stones or encrustations that foul devices, such as urinary stents[244]. Mucosal surfaces also experience a wider range of pH values than skin, for example, in the GI tract, the pH varies from low values (pH 1.2–3) in the gastric cavity to higher values in the intestines (pH 5–7)[236].

In other respects, mucosal surroundings are subject to less environmental fluctuation than skin. For example, skin temperature varies with its surroundings, but mucosal temperatures are largely maintained around core body temperature, although they can increase slightly with exercise and infection, and exhibit variability in regions closest to external orifices, such as the oral cavity[245]. Additionally, gas compositions in the mucosal lumen can differ from those in contact with the skin. For example, oxygen content in mucosal lumen is usually lower than that in atmospheric air, whereas gases such as carbon dioxide, hydrogen and hydrogen sulfide are generated from endogenous biochemical processes related to digestion[246], sugar fermentation in urine[247] and pregnancy[248], respectively.

Interplay between microorganisms and mucosa is important in the inner body. For example, vaginal homeostasis is maintained by endogenous lactobacilli, which are nourished by glycogen deposits in the epithelium and help maintain a low vaginal pH (<4.5)[249]. Bacteria in the digestive tract also support digestion[250], defence[250] and immunity[251]. Even the lungs house a diverse microbiome that both influences and is responsive to immune responses and inflammation[252].

Sensing functions

On skin, physical signals like pressure and temperature are transduced into electrical signals by the sensory receptors (the exteroreceptors)[9], such as mechanoreceptors[253]. Conversely, mucosa host a set of additional sensory receptors (the interoceptors) that pertain to specific organ functions and sensitive responses of the inner body. The afferents in the oesophageal mucosa are sensitive to multiple chemicals (such as hypertonic saline, sodium hydroxide and serotonin) that regulate collective muscular motions to advance food and prevent backflow[254]. Taste receptors have been found in parts of the inner mucosa[255]. For example, bitter taste receptors on epithelial cells lining the airways, gastric mucosa and bladder induce purging mechanisms for clearing gas and fluid upon activation[255]. The vesical mucosa has many mechanoreceptors and pain receptors for signalling the urge for urination, but about 30% of the total afferents are 'silent' and only develop partial responses to mechanical stretching after acute inflammation of the bladder[256].

Table 1 | **Diagnostic opportunities of the mucosa categorized by different conditions**

Key opportunities	Current clinical approaches	Mucosal signals with potential diagnostic value
Reproductive tract		
Conception and fertility planning and management	Body temperature measurement; qualitative inspection of vaginal mucosa; digital pelvic exam	Mucosa properties: vaginal mucus impedance, stiffness and viscosity Temperature: real-time monitoring of basal body temperature Biochemical: uterus pH and oxygen levels Mechanical: pressure-based detection of cervical tenderness, uterus size and uterus stiffness Electrical: measuring uterine contractile activity to predict delivery time and identify abnormal labour
Reproductive cancer	Tissue biopsy	Biochemical: protein biomarkers associated with different cancers; DNA and RNA sensors for detecting mutations and viral infections associated with cancers (for example, HPV)
Dysbiotic environments associated with infection	Digital pelvic exam; imaging vaginal secretions; vaginal pH measurements	Biochemical: vaginal pH levels; quantity and diversity of bacteria in vaginal flora
Urinary tract		
Urinary incontinence and overactive bladder	Self-reporting; post-void residual measurement	Mechanical: bladder pressure and strain detection Electrical: impedance measurements of bladder volume; electrophysiological indicators of bladder disease
Acute kidney injury	Blood panel; cytology and evidence of casts (aggregates of cells)	Biochemical: creatine detection in kidneys Mechanical: direct measurement of pressure and strain exerted on kidneys
Bladder cancer	Cytology evaluation using cystoscopy	Biochemical: urine protein biomarkers Mucosa properties: colour abnormalities in bladder mucosa
Kidney stones	Blood panel; urinalysis; imaging	Biochemical: Ca levels in kidneys; mineral levels, white blood cells and bacteria in urine
Digestive tract		
GERD	Endoscopy and imaging; ambulatory acid (pH) test; oesophageal manometry	Mucosa properties: oesophageal mucus impedance Biochemical: oesophageal pH level; cell-type evaluation Electrical: impedance measurements of luminal content
GI motility disorders	Endoscopy; *Helicobacter pylori* (breath) test; stool test	Electrical: EGG; slow-wave activity Mechanical: pressure recording in GI tract Biochemical: pH and gas in stomach and Ca^{2+} in intestines
GI cancer	Tissue biopsy; endoscopy or colonoscopy; imaging	Biochemical: protein, DNA or RNA biomarkers associated with GI cancers Mucosa properties: elastic modulus of stomach for gastric cancer; hardness of colon for colorectal neoplasms
Peptic ulcer	Endoscopy; imaging; *H. pylori* tests	Mucosa properties: mucosal quality and elastic modulus for *H. pylori*-related gastric and duodenal ulcers Biochemical: protein, DNA or RNA sensors for detecting bacterial infections associated with ulcers (for example, *H. pylori*) Vascular dynamics: GI mucosal blood flow
GI inflammation (for example, gastritis and IBD)	*H. pylori* tests; stool or blood test; imaging; endoscopy or colonoscopy	Mucosa properties: mucosal integrity, impedance, stiffness Biochemical: protein, DNA or RNA sensors for inflammation-relevant biomarkers; sensing of macronutrients or metabolites levels Vascular dynamics: GI mucosal blood flow
GI ischaemia	Imaging	Vascular dynamics: GI mucosal blood flow Biochemical: oxygen sensing for intestinal oxygen tension
Gut–brain axis	Intravital Ca^{2+} signal imaging of the gut	Electrical: electrophysiology Biochemical: neurotransmitter sensing (for example, dopamine) in the gut
Respiratory tract		
COPD and cancer	Pulmonary function tests; chest imaging; arterial blood gas analysis; spirometry; tissue biopsy	Mechanical: monitor pressure within lung and bronchial airflow Biochemical: protein, DNA or RNA sensors for disease-relevant biomarkers; pulmonary oxygen levels Vascular dynamics: arterial blood vessel diameter; blood pressure of femoral artery Mucosa properties: modulus of bronchial airway walls; stiffness of trachea rings

Table 1 (cont.) | **Diagnostic opportunities of the mucosa categorized by different conditions**

Key opportunities	Current clinical approaches	Mucosal signals with potential diagnostic value
Respiratory tract (cont.)		
Tuberculosis	Physical exam; blood, skin or sputum tests; imaging	Biochemical: protein, DNA or RNA sensors for detecting MTB
Asthma	Physical exam; spirometry; exhaled nitric oxide test	Mechanical: pressure within lung and bronchial airflow Mucosa properties: pulmonary mucus impedance, viscosity, colour
Pneumonia	Physical exam; blood or sputum tests; imaging; pulse oximetry; RT-PCR	Mucosa properties: pulmonary mucus impedance, viscosity, colour Biochemical: protein, DNA or RNA sensors for detecting viral infections associated with pneumonia (for example, SARS-CoV-2, MERS and SARS in respiratory mucus); oxygen levels

COPD, chronic obstructive pulmonary disease; EGG, electrogastrogram; GERD, gastro-oesophageal reflux disease; GI, gastrointestinal; HPV, human papillomavirus; IBD, inflammatory bowel disease; MERS, Middle East respiratory syndrome; MTB, *Mycobacterium tuberculosis* bacteria; RT-PCR, reverse transcription polymerase chain reaction; SARS, severe acute respiratory syndrome.

diagnostics can help to support screening for colorectal, oesophageal, lung, urinary tract, cervical, endometrial and ovarian cancers[25,26].

Clinically available mucosal biochemical diagnostics are limited. For reproductive health, self-testing kits are available, namely, vaginal swabs that are used to measure pH and diagnose conditions such as bacterial vaginosis outside of the clinic[27]. Oesophageal manometry can be upgraded to include pH sensing to diagnose diseases such as gastro-oesophageal reflux disease. Such diseases can also be diagnosed using the Bravo reflux testing system, which is a capsule-based method that evaluates pH for up to 96 h in the lower oesophagus[28]. The Atmo ingestible gas capsule senses oxygen, hydrogen and carbon dioxide during GI transit to provide unique insight into GI disorder pathogenesis[29]. Beyond these examples, physicians still largely rely on conventional diagnostic techniques such as blood and bodily fluid panels for biochemical analysis, whereas tissue biopsy remains the gold standard for cancer diagnosis. In addition to being limited to hospital settings, these tests typically require long wait times to obtain results, precluding real-time or long-term monitoring.

Temperature

Body temperature is one of the most straightforward indicators of metabolic state and health status. Normal human body temperature is often reported as 36.5–37.5 °C, but depends on measurement location and time[30]. Infection and inflammation usually induce fevers. Food and drink intake patterns result in gastric temperature fluctuations of up to 4 °C (REFS.[31,32]), which could be applied to quantitatively evaluate dietary habits[33]. Temperature changes measured within the urinary bladder are more closely correlated to pulmonary artery temperature and, therefore, to core body temperature, than are recordings performed in the rectum or on skin[34]. Basal body temperature is also highly correlated with menstrual cycle stages and can be used to track fertility, with most women experiencing a slight temperature increase during ovulation[35,36].

Currently, several techniques are available to monitor body temperature through the mucosa or lumen. Temperature measurements within the oral cavity and rectum are the clinical norm for fever monitoring. Urinary bladder temperature monitoring through indwelling urinary catheters is commonly used and considered as the reference method, especially in intensive care units[34,37].

Outside of clinical settings, ingestible capsules such as e-Celsius and SmartPill can wirelessly measure the core temperature as they pass through the GI tract. OvulaRing, a vaginal ring with an integrated thermometer and wireless readout that can be retained in the reproductive tract, is a commercial product used to forecast ovulation more accurately than daily self-measurements of basal temperature, especially for women with menstrual cycle irregularities[36]. Its ability to continuously monitor temperature with regional specificity is an exciting demonstration of the benefits of a long-term MIE device.

Vascular dynamics

Submucosal vascular dynamics, or haemodynamics, are receiving increasing attention for their ability to predict pathologies and abnormal healing. Mucosal blood flow has an important role in healing gastric ulcerations, as blood flow around ulcers should increase during normal healing[38,39], and intestinal ischaemia occurs when blood flow through the major arteries that supply blood to the intestines becomes restricted. Additionally, pulmonary microvascular and macrovascular dynamics are correlated to the evolution of conditions such as chronic obstructive pulmonary disease[40], whereas bladder haemodynamic measurements can enable earlier treatment of lower urinary tract diseases[41]. Finally, abnormalities in ovarian arterial blood flow to the reproductive tract may predict complications during late pregnancy[42], whereas a change in renal blood vessel diameter may indicate impending kidney failure.

Current clinically available haemodynamic measurements are mainly dependent on optical methods (such as photoplethysmography and laser Doppler flowmetry), sphygmomanometry and ultrasound imaging. Ultrasonic and optical techniques have been combined with bronchoscopy, endoscopy or colonoscopy to monitor the haemodynamics of difficult-to-reach mucosa-lined organs (for example, the stomach, bowels and lungs)[43,44]. Endoscopic Doppler optical coherence tomography acquires high-spatial-resolution velocity-variance images of GI mucosal and submucosal blood flow. Endobronchial ultrasound bronchoscopy is a

minimally invasive procedure used to provide real-time imaging of the surface of airways, blood vessels, lungs and lymph nodes to diagnose lung cancer and chest infections[45]. These techniques are all mainly performed in hospitals, require uncomfortable pre-procedure preparations (such as fasting and sedation), can cause post-procedure infections and are not ideal for long-term monitoring owing to either their bulky size or short retention time.

Mechanical signals

Mechanical signals within mucosa-lined regions are highly correlated to health. For example, airway pressure drops abnormally for patients with trachea and bronchial stenosis[46]; oesophageal pressure is related to the motor function of oesophageal muscle contractions; slow whole-gut transit time could be caused by gastroparesis[47], functional dyspepsia[48], inflammatory bowel disease and intestinal paralysis; lumen pressure and strain are the best direct indicators of bladder function[49]; and abnormalities in vaginal wall biomechanics during pregnancy could be early indicators of miscarriage, ectopic pregnancy or preterm labour[50].

Manometry (anorectal, oesophageal and gastroduodenal) measures pressure within the GI tract. The ingestible SmartPill motility capsule is a promising advance from traditional tethered manometry that can localize transit abnormalities to specific GI regions. In the respiratory system, airway pressure is clinically monitored with ventilators, but manometry could be an alternative solution[51]. Digital pelvic exams are standard for vaginal pressure monitoring; submucosal bladder pressure monitoring is feasible but still technically challenging[52]. Although manometry is generally safe, patients can experience some discomfort and existing techniques lack long-term monitoring capability.

Mucosal properties

Changes in mucosal properties such as colour, texture, stiffness and hardness are indicative of pathological conditions. For example, GI tissue infected with *Helicobacter pylori* is softer than normal[53], whereas cancerous mucosa is harder[54]. Chronic respiratory airway injury can manifest in epithelial denudation, mucosal ulceration, subepithelial thickening, collagen deposition and increased stiffness[55,56]. In patients with various bladder diseases, mucosal colour changes often precede lesions, followed by contour changes in the bladder[57]. Vaginal wall tissue stiffness in women with pelvic organ prolapse is also higher than that measured prior to prolapse[58,59].

Standard clinical evaluation of mucosal properties depends on palpation, imaging and tissue biopsy. Palpation is a common but subjective method for diagnosing mucosal abnormalities in the oral cavity, rectum and vagina. Endoscopic imaging has been clinically implemented to investigate mucosal integrity and colour in the GI tract, bladder and lungs, and computed tomography imaging can be used to diagnose pulmonary cystic fibrosis by identifying abnormal mucus and dilated airways in the lungs[60]. In a move to reduce invasiveness, ingestible capsules such as the PillCam directly visualize the small bowel and colon and their related lesions[61]. However, imaging cannot examine deep mucosal layers, where precancerous property changes often occur[53]. Finally, endoscopy can be used to collect tissue biopsies, although samples are analysed ex vivo and may require long processing times. Although useful, endoscopy in general requires burdensome pre-procedure preparations, such as fasting, bowel preparation (cleansing) with laxatives and sedation, and can be associated with periprocedural complications[62].

Environmental signals

As the inner skin of the body, the mucosal lining is continuously exposed to exogenous sources such as drugs[63], contaminated food[64] or sexually transmitted viruses[65]. Currently, clinical diagnostics are implemented only after symptoms arise. For example, contaminated foods usually cannot be detected in advance, and blood or stool tests diagnose digestive infections only after they have become symptomatic. Mucosal devices capable of detecting environmental pathogens in real time could enable a transition from a reactive to a proactive framework for disease management, which could dramatically improve quality of life and health outcomes.

Towards mucosa-interfacing electronics

The above discussion demonstrates the need to develop electronics for minimally invasive, real-time, continuous and untethered sensing from the mucosa to aid the management of a broad array of conditions by increasing the diagnostic accuracy, enabling faster response times and expanding accessibility to broader patient populations. Despite these promising opportunities, major hardware challenges exist that arise from the unique anatomical and physiological features of mucosa-lined organs, leading to large technological gaps between SIE and MIE. These issues can be grouped into two overarching challenges. First, the mucosal environment is generally more physically and biochemically extreme than that of the skin. Specifically, mucosa is highly curvilinear and includes regions of large spontaneous motion, such as peristalsis, making it difficult to establish robust sensor–tissue interfaces and to achieve long-term retention. Additionally, the mucosa surface is wet and dynamic with high cellular turnover and is often exposed to large amounts of exogenous and endogenous matter, posing challenges for device encapsulation and retention. Second, accessing the mucosa is non-trivial compared with accessing skin, presenting unique challenges in terms of device delivery and removal, as well as with powering the device and communicating with it to extract the recorded data.

In this section, we present the materials and device engineering challenges for realizing MIE and discuss potential solutions. Many of these solutions are inspired by advances in SIE and other types of bio-integrated electronic systems, which have long grappled with similar challenges, such as achieving reliable interfacing with soft and dynamic bodily surfaces to obtain high signal fidelity[66–68]. However, careful design considerations are needed to interface electronics with the mucosa owing to additional complications related to the anatomy, physiology and biochemical environments of mucosa (FIG. 2).

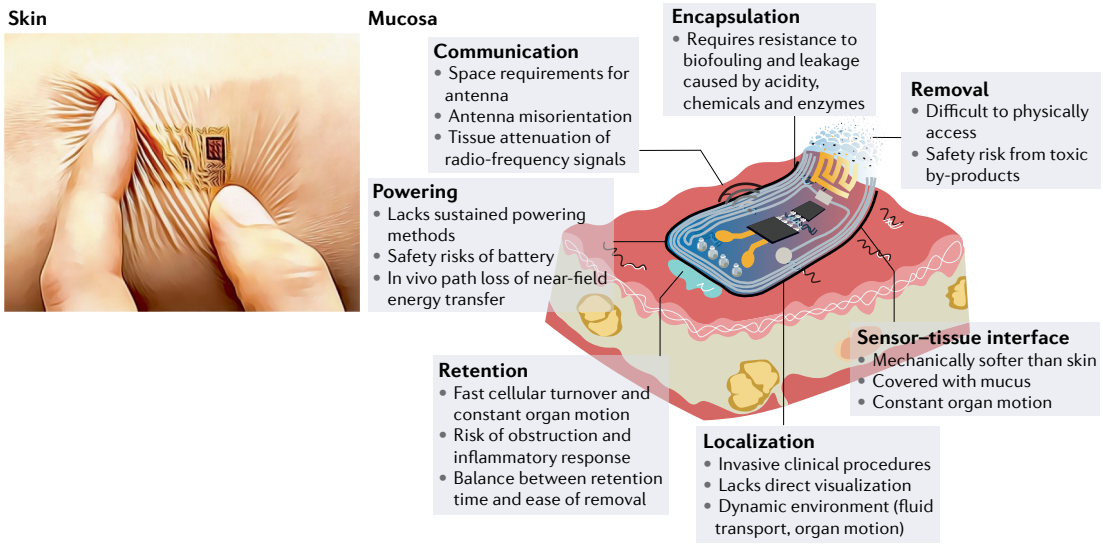

Fig. 2 | **Towards mucosa-interfacing electronics.** Schematic of an envisioned mucosa-interfacing electronics system, outlining the main challenges facing mucosa-interfacing electronics devices (right) compared with state-of-the-art skin-interfacing electronics (left). The challenges include aspects related to sensor performance (sensor–tissue interface and encapsulation), sensor deployment (localization, retention and removal) and communication and power supplies. Left image courtesy of J. A. Rogers.

Signal acquisition

Establishing a sensor–tissue interface with mucosa. Non-invasive, continuous and long-term sensing in the mucosa requires a chronically stable and robust sensor–tissue interface, which is primarily challenged by the mechanical mismatch between rigid electronics and soft mucosa[69]; the presence of a slippery mucus layer; and constant perturbation by dramatic organ motion, such as peristaltic motion in the digestive tract. The two main strategies that have been extensively explored in the field of SIE (that is, structural and materials engineering; FIG. 3a) show promise at establishing robust interfaces even in these difficult environments. Many soft surface electrodes have been used as minimally invasive, chronic sensor–tissue interfaces (TABLE 2).

Structural engineering strategies have been used to obtain flexible and stretchable electronics, including battery arrays[70] and integrated circuits[71], for long-term conformal contact with the body. To strengthen the van der Waals forces between the device and the tissue, the electrode dimensions can be reduced to sub-micrometre thickness with a low-filling-ratio configuration using advanced photolithography[72,73]. In the digestive tract, flexible sensors with sub-millimetre thickness have shown adhesive-free attachment onto the gastric mucosa of anaesthetized animals to record electrophysiological and mechanical signals[74,75], although their effectiveness in freely moving animals over long time frames remains to be tested.

Structural engineering approaches achieve stretchability through an island–bridge configuration[76], in which electronic components that are common in rigid sensory circuits and microelectromechanical systems are arranged into sparse arrays ('islands') on soft substrates and connected using stretchable conductors, such as carbon-black-doped silicone[77] or liquid metals[78] ('bridges'). Non-stretchable materials such as metals and conductive pastes can also be converted into stretchable interconnects by patterning them into architectures that include self-similar serpentine traces[79], wrinkles[80], 3D arcs[81] and helices[82], kirigami-inspired cutting patterns[83] and textiles[84] (FIG. 3b).

Materials engineering approaches, by contrast, employ intrinsically soft and stretchable materials that retain their electronic properties under large deformations, such as conjugated polymers[85], liquid metals[86] and composites of elastomers[80], as well as functional nanomaterials[87] that can be patterned into high-density transistor arrays (up to 347 transistors per cm^2)[88,89]. Sensor–tissue interfaces that achieve long-term (up to several months) interfacing with various organs in vivo have been demonstrated[75,77,90,91]. For example, low-modulus silicone-based elastomers were used to engineer a soft (elastic modulus < 70 kPa) and elastic strain gauge that can be worn over the urinary bladder peritoneum to repeatedly measure its expansion and contraction in real time, while only exerting <2% compressive strain on the bladder[77]. Similar techniques led to the development of NeuroString, an ultra-soft electrochemical sensor made of porous graphene electrodes and elastomeric encapsulations, which was used to demonstrate, in acute settings, stable interfaces with the rodent GI mucosa for simultaneous tracking of dopamine and serotonin levels[92].

Conductive hydrogels are promising candidate materials for establishing compliant, robust and stable sensor–tissue interfaces with the mucosa, owing to their tissue-like softness (elastic modulus < 500 kPa) and high water content (>70%). The mechanical properties of hydrogels such as viscoelastic moduli, viscoplasticity and stretchability can be tuned to match those of target tissues by adjusting the polymer chemistry, molecular weight and crosslinking density of the hydrogel[93,94]. Hydrogels can also enhance electrical coupling at the

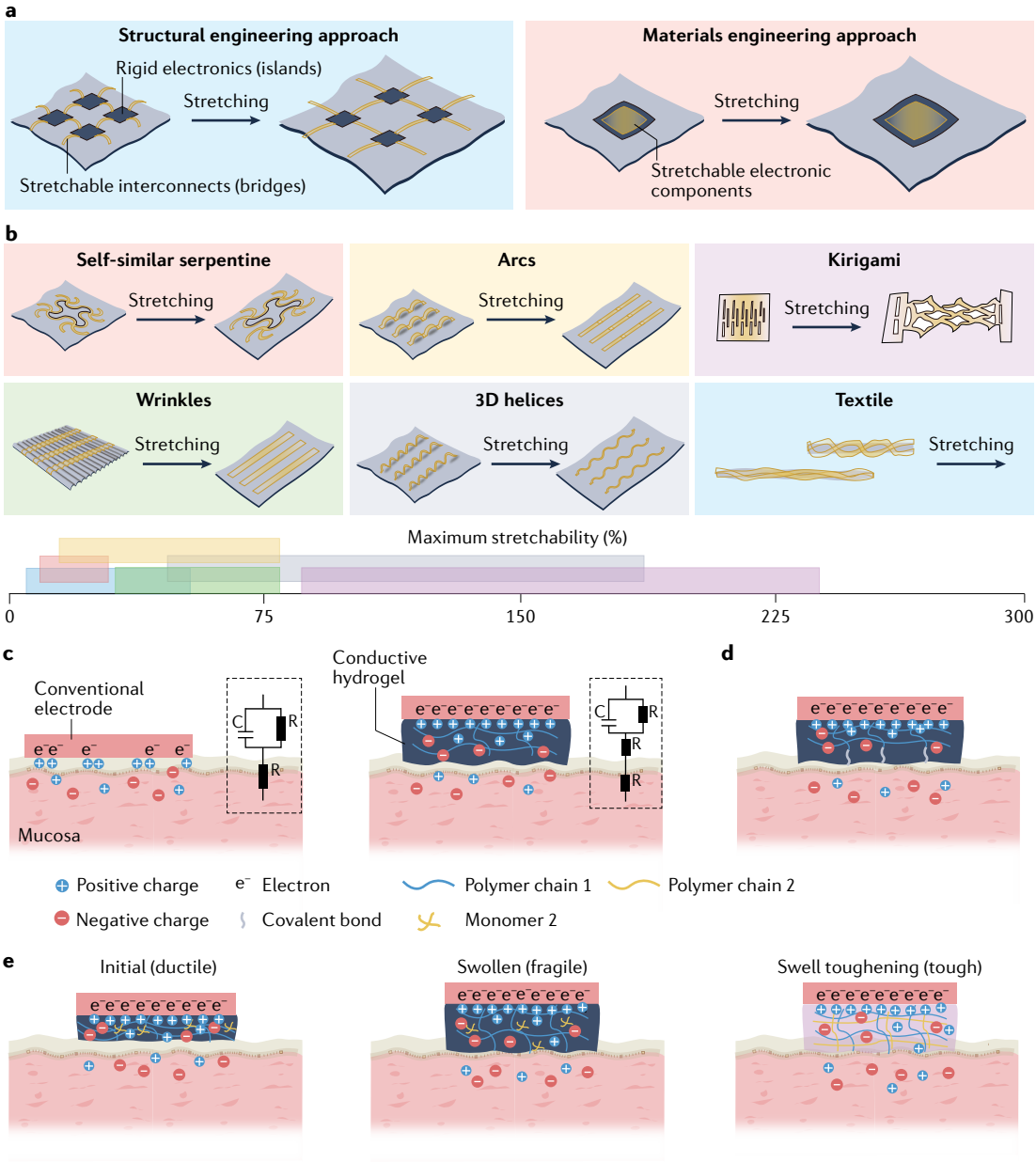

Fig. 3 | **Methods for establishing sensor–tissue interfaces with mucosa. a** | Illustration of the structural (left) and materials (right) engineering approaches for establishing robust sensor–tissue interfaces. **b** | Schematics of various structural engineering approaches that convert plastic materials into stretchable conductors, showing the conductors before and after stretching. The axis shows a range of reported maximum stretchability for each approach. **c** | Schematic showing the enhancement of the sensor–tissue interface by minimizing the mechanical mismatch with the tissue using a soft hydrogel (right) compared with a sensor–tissue interface with a conventional electrode (left). The insets show the corresponding equivalent circuit diagrams, comprising capacitors (C) and resistors (R). **d** | Schematic showing the formation of covalent bonds between a conductive hydrogel and tissue to simultaneously realize strong adhesion and low electrical impedance at the sensor–tissue interface. **e** | Schematics showing the initial hydrogel (left), the fragile swollen state of the hydrogel following fluid uptake (middle) and the swelling-triggered toughening mechanism that involves the diffusion of encapsulated crosslinker molecules in the first polymer network (polymer 1) and then crosslinking of a second polymer network (polymer 2) to enhance the toughness of the hydrogel after fluid uptake (right).

sensor–tissue interface. By minimizing the mechanical mismatch between the device and the tissues compared with conventional electrodes, hydrogels also eliminate the tiny voids that typically increase interfacial impedance at the sensor–tissue interface (FIG. 3c). Furthermore, hydrogels conduct electricity using ions and have similar conductivities to those of biological tissues ($0.1–10\,S\,m^{-1}$)[95,96]. For instance, poly(vinyl alcohol)-based hydrogels with 88 vol% saline support tissue-like ionic conductivities of $0.3–0.5\,S\,m^{-1}$ at 1 kHz to enable high signal-to-noise ratios of 20 and 30 dB for electrocorticography in rat and porcine brains, respectively[97]. Conjugated polymer-based hydrogels with mixed electronic and ionic conductivities also

reduce the interfacial impedance at frequencies below 1 kHz (REF.[98]).

A new group of hydrogel-based sensor–tissue interfaces exploits hydrogels with both conductive and tissue-adhesive features to simultaneously realize strong bonding and low electrical impedance at the sensor–tissue interface (FIG. 3d). For example, advances in photocurable conductive hydrogel bioadhesives have enabled the adhesion of devices onto wet tissues with electrical conductivities of ~1 S m^{-1}, while the optical transparency enables wireless phototherapy to treat neurological disorders[99]. Graphene-incorporated conductive hydrogel bioadhesives (with conductivities of 2.6 S m^{-1}) have been exploited for long-term electrocardiography recordings on the surface of a rodent heart[100].

Although hydrogel-based sensor–tissue interfaces that are stable for up to 1 month have been realized on the outermost surfaces of the heart[101,102], lungs[101] and intestinal serosa[103,104], their long-term performance on the mucosa remains unclear. Limitations arise owing to the intermittent flow of bodily fluid and fast cellular turnover of mucosal epithelia[105]. Janus hydrogel patches with omniphobic luminal-facing surfaces demonstrated extended GI retention by repelling the food and fluid streams[106]. Strategies that bypass mucosal epithelia by directly accessing the underlying tissues have also been explored to enhance the longevity of the sensor–tissue interface. A promising approach is to exploit the bonding of the hydrogel with tissue-specific or cellular-specific sites on selected mucosal tissues and cells[107,108] that have much slower turnover rates. For instance, a genetically targeted approach was used to demonstrate the in situ assembly of conductive polymers on electrically active cells in neural tissues[109]; this method can potentially be adapted to establish low-impedance electrical interfaces at target cell types with slower turnover rates in the mucosa.

Zwitterionic hydrogels, which are crosslinked polymeric networks that contain equal numbers of cationic and anionic groups, are great matrix materials for hydrogel-based sensor–tissue interfaces owing to their antibacterial and anti-biofouling properties and their ability to attenuate immune responses[110]. For example, ultra-low-biofouling zwitterionic hydrogels can resist fibrotic capsule formation for at least 3 months after subcutaneous implantation in mice, while promoting angiogenesis in the surrounding tissue[111]. These features result partly from the more densely bonded hydration layers and less orientated water molecules in zwitterionic hydrogels than in traditional hydrogels.

Table 2 | **Recently reported surface electrodes as minimally invasive, chronic sensor–tissue interfaces**

Sensor material	Substrate material	Fabrication methods	Total thickness (μm)	Bending stiffness (nN m)	In-plane stretchability (%)	Electrical conductivity (S m^{-1})	Interfacial impedance at 1,000 Hz (Ω)	Targeted organ (duration)
Au (REF.[225]), Pt (REFS.[72,73]) or PEDOT-coated Pt (REF.[226])	Polyimide[225], SU-8 (REFS.[72,73,226])	Photolithography, thin-film transfer	0.4–1	~5 × 10^{7}–1	<10 (REFS.[72,73]), 30 (REF.[226])	9.4 × 10^{6} (Pt), 4.5 × 10^{7} (Au)	10,000–60,000	Human skin (24 h)[225], rat brain (12 weeks)[72], mouse retina (14 days)[72,73], human cardiac organoid culture (40 days)[226]
W-coated Mg (bioresorbable)[227]	PLGA (bioresorbable)[227]	Photolithography, thin-film transfer	250	15,000	<10	8.9 × 10^{6} (W), 2.2 × 10^{7} (Mg)	NA	Dog heart (dissolved after 4 days)[227]
Au nanofibres[228], Au nanomesh[229]	Parylene C	Electrospinning	0.1–0.5	~0.1–1	30	2 × 10^{6}	50,000	Human skin (7 days)[228], human cardiomyocytes culture (4 days)[229]
Conductive hydrogel adhesives[99,100]	None	Casting	100–500	~1	200 (REF.[100]), 1,300 (REF.[99])	0.5 (REF.[99]), 2.6 (REF.[100])	50 (REF.[100]), 10,000 (REF.[99])	Rat brain and heart (2 months)[99], rat heart and tendon (14 days)[100]
PEDOT:PSS with ionic liquid[230], with glycerol (for viscoplasticity)[91] and with polyrotaxanes (for enhanced stretchability)[217]	PDMS[91,230], SEBS[217]	Photolithography	1–100	~1 × 10^{-6}–0.1	20 (REF.[230]), 100–150 (REFS.[91,217])	200 (REFS.[91,230]), 1 × 10^{4} (REF.[217])	50 (REF.[217]), 6,000 (REF.[91]), 50,000 (REF.[230])	Rat sciatic nerve (2 months)[91], pig heart (acute)[230], rat brain (acute)[217]
Hydrogel with conductive carbon fillers[90] or PDMS with Pt nanoparticles[231]	PDMS	Moulding and casting	60–100	~0.1	45 (REF.[231]), 1,000 (REF.[90])	10 (REF.[90])	5,000–10,000	Rat heart, tendon and brain (acute)[90], rat brain and sciatic nerve (6 weeks)[231]

NA, not available; PDMS, polydimethylsiloxane; PEDOT:PSS, poly(3,4-ethylenedioxythiophene) polystyrene sulfonate; PLGA, poly(lactic-*co*-glycolic acid); SEBS, styrene–ethylene/butylene–styrene.

A key challenge of using traditional zwitterionic hydrogels as sensor–tissue interface materials is their low mechanical toughness, which can be addressed by incorporating another polymeric network, such as chitosan, into the hydrogel[112].

One of the limitations of using hydrogels as sensor–tissue interfaces is the loss of mechanical toughness and integrity caused by hydrogel swelling. Coatings made of compatible elastomers can reduce the fluid uptake rate of the hydrogel[113] and toughening can be achieved through swelling-triggerable crosslinking of a second polymer network[114] (FIG. 3e). Another major challenge associated with using hydrogels is the weak bonding of conductive hydrogels to other device components, particularly to commercially available metal electrodes and connectors for establishing external electronic connections. A promising solution involves using surface functionalization chemistry to graft a hydrophilic adhesive layer onto the target surface, which can then be strongly adhered to the conductive hydrogel owing to the interpenetration of the polymer chains[115].

Biochemical sensing. Biochemical sensing in mucosal environments poses additional challenges compared with sensing on skin. For example, real-time sensing is complicated by typically small analyte concentrations. To amplify signals, MIE can learn from skin-interfacing microfluidic systems that use long microfluidic channels to allow sufficient volumetric contact between the analyte and the electrodes with specific surface functionalization for biomarker detection[116,117].

Active sensor components must also withstand the reactive environment, which can be challenging in regions like the acidic stomach cavity. Promising solutions include the use of waterproof interfaces, inspired by the use of sweat collection interfaces made from poly(styrene-isoprene-styrene) in SIE to withstand swimming and showering[118], and the use of inherently resilient active components, such as acid-resilient sensing bacteria[119].

Additionally, biochemical sensors must maintain selectivity for the target analyte, which can be achieved by identifying specific electrochemical fingerprints using aptamers that interact only with the target molecule[120]. Gas-sensing ingestible capsules have also been developed using membranes that effectively block out liquids while enabling fast diffusion of gases such as H_2 and CO_2 into the device[29]. This technology could potentially be leveraged for the diagnosis of GI motility disorders[121] or intestinal ischaemia[122], which are both associated with changes in intestinal gas content. For liquid sensing, membranes with high selectivity can be realized using molecular imprinting, which moulds the membrane pore structure around the analyte of interest[123]. Although molecularly imprinted sensors have not yet been used for mucosal sensing, they have been effectively used for both wearable and implantable applications[124].

Encapsulation and biofouling. Encapsulation materials that insulate electrodes from the surrounding environment are crucial for extending the longevity of electrical connections and minimizing sensor crosstalk. Nano-thin inorganic films (such as Al_2O_3, HfO_2, SiO_2 and SiC) offer bending flexibility and demonstrate in vivo biofluid-sealing abilities that are superior to those of their organic thin-film counterparts such as polydimethylsiloxane[125], but the presence of surface defects during oxide formation leads to low fatigue resistance against the constantly moving mucosal tissues. An interesting concept is to exploit bio-inspired, nano-textured surfaces[126] or a layer of oil locked onto or within a rough and porous elastomer matrix[127] as superhydrophobic barriers against biofluid. Fluorinated synthetic oil has excellent barrier properties against hydrochloric acid[127], suggesting that it could be used for long-term encapsulation in low-pH environments like the stomach.

Additionally, biofouling of sensors and device components, which leads to signal drift or loss of functionality, is a particular concern in mucosal environments, which regularly encounter exogenous debris[128]. Beyond the poly(ethylene glycol) and zwitterionic coatings commonly used to reduce biofouling, combinatorial screening approaches have also yielded promising candidates for coating implantable biosensors, including certain copolymers with acrylamide, which could be used in the future to address biofouling in different mucosal environments[129].

Modes of retention on the mucosa

Retention of MIE in a minimally invasive (without surgery), safe (without perforation and obstruction) and chronic (weeks to months) manner presents a major hurdle owing to continuous cellular turnover, the presence of mucus layers, intraluminal fluid shear effects and organ motion[130]. To extend retention, several approaches exist that leverage modes of interaction at different levels of proximity to the mucosa (FIG. 4). Strategies capable of maintaining devices in direct contact with the mucosa are ideal for accessing the myriad signals, although long-term interfacing is challenging owing to cellular turnover. In general, adhesive strategies that incorporate mechanisms to penetrate the outermost mucus layer and establish contact with epithelial cells that have lower turnover rates will likely have optimal performance for achieving both high signal fidelity and chronic retention.

Mucus-adhering strategies. Several mucus-adhering (mucoadhesive) materials have been developed that use chemical and physical interactions to prolong retention on the outermost mucus layer (FIG. 4a), which is a water-rich viscoelastic gel that comprises up to 5% of the glycoprotein mucin[131]. Typical mucoadhesive mechanisms involve non-covalent interactions, such as hydrogen bonding, hydrophobic interactions, electrostatic interactions, mechanical interlocking and interdiffusion of polymer chains; the efficacy of these interactions also depends on surface properties, such as roughness, and the ability to move water away from the hydrated mucus interface[131]. Mucoadhesion can be further strengthened through the formation of covalent bonds, for instance, by reactions between alkene groups and the thiol groups present in the cysteine residue of mucin[131], or by incorporating microsized and nanosized

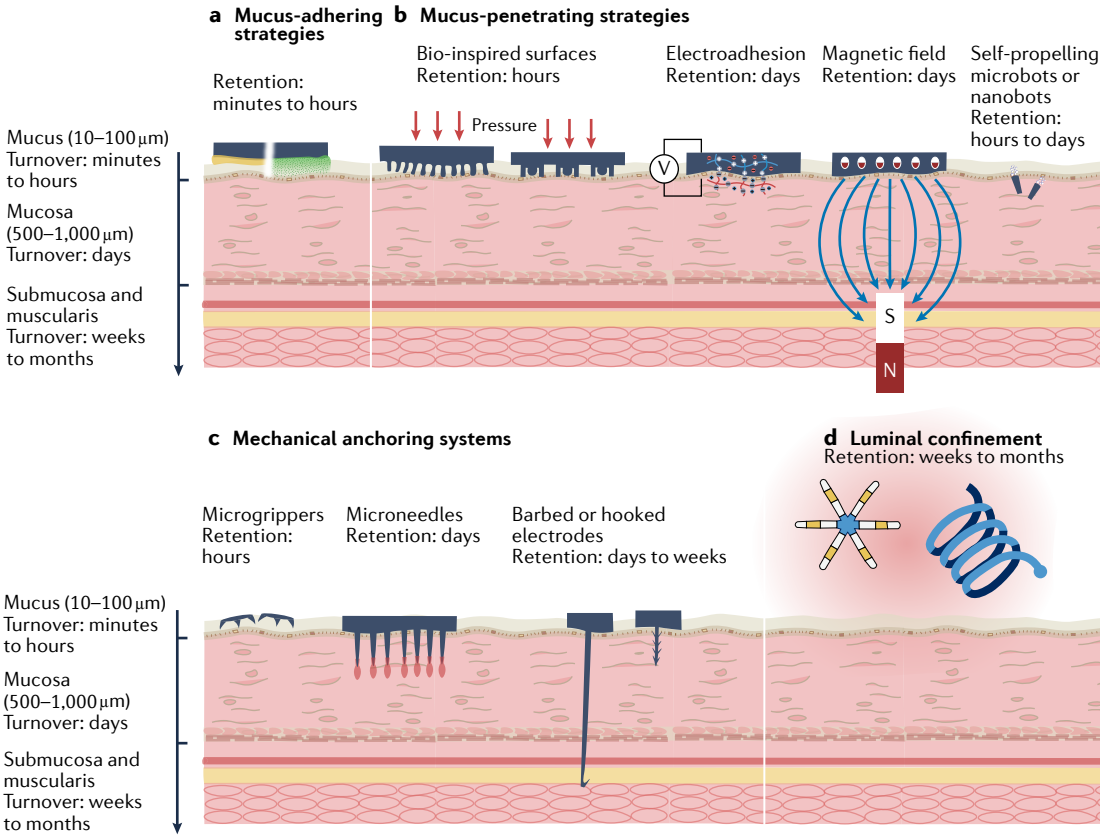

Fig. 4 | **Modes of retention on the mucosa.** Different physical and chemical adhesive mechanisms (mucus-adhering (part **a**), mucus-penetrating (part **b**), mechanical anchoring (part **c**) and luminal confinement (part **d**) strategies) lead to a wide range of average retention times from minutes to months. In general, methods that penetrate or deplete the mucus and interact directly with the underlying mucosa offer longer retention, but at the expense of increased invasiveness. Luminal confinement provides the longest retention.

particles into adhesives to increase the surface area-to-volume ratio of the mucoadhesive materials[132]. Existing mucoadhesive materials are primarily used for prolonged drug delivery at various sites of action, including the nasal cavity[133], vaginal lumen[134] and digestive tract (for example, the oral cavity[135,136], intestinal lumen[137,138] and colon[139,140]).

These mucoadhesive strategies can increase the retention time of devices on the outermost surface of the mucosa to several hours, which may be sufficient in some cases to improve signal collection at the mucosal interface. However, for theranostics that rely on chronic retention on the order of weeks or months, surface adhesion is generally insufficient owing to the relatively rapid turnover of the mucus layer.

Mucus-penetrating strategies. To achieve both prolonged device retention and high signal fidelity, adhesive mechanisms that penetrate the mucus to interact with the underlying mucosal epithelium (FIG. 4b), which comprises cell types with a much slower turnover, are being pursued. The retention time and mucus penetration depth of microparticles or nanoparticles can be increased by engineering mucus-penetrating particles, which are a type of nanoparticles with non-mucoadhesive surfaces and particle diameters that are smaller than the mucus mesh (for example, 20 nm for the cervix and 500 nm for the stomach[141]). Mucus-penetrating particles can avoid being trapped by the innermost mucus layer and freely diffuse into deeper mucosal epithelium, achieving longer retention time, for example, 12–24 h in the intestine and colorectum[142,143], up to 36 h in the stomach[144], up to 24 h in vaginal folds[145] and up to 24 h in the lungs[143]. Animals that possess unique body features[146,147] to enable adhesion in wet conditions have inspired mechanisms to facilitate device adhesion to the mucosa beneath the mucus layer. These features include high-density, large-surface-area arrays of nanoscale or microscale patterns, as has been used in octopus-inspired suction cups[148] and gecko-inspired micropillars[149,150], which both require only mild pressures to deplete the water-rich mucus layer and activate intimate physical contact with the underlying mucosa, and can be further functionalized with other mucoadhesives (for example, with mussel-inspired catechol adhesives)[104] to prolong retention. A potential advantage of these systems is their compatibility with scalable fabrication technologies (such as moulding, spin coating and drop casting), which yield standalone films for subsequent integration with electronics in thin-film configurations. On the macroscale, fabrication techniques such as multi-material 3D printing have also been used to create devices with bio-inspired adhesive features, including a remora-inspired soft robot with

hydraulically actuated silicone lamella that reversibly adheres to wet surfaces[151].

Mucus penetration and depletion can also be achieved by manipulating the charge of the polymer chains to drive their diffusion through the mucus layer. Tissues typically consist of polycationic or polyanionic chains. For example, the surface mucosa that lines the stomach and intestines is predominantly negatively charged[152,153], which facilitates penetration of positively charged polymers so that covalent amide bonds can be formed with the underlying mucosa[102]. However, the long diffusion time (~30 min)[102] is not ideal for clinical translation. Applying an external electric field accelerates this process so that polyelectrolytes can penetrate the mucus to the underlying mucosa within seconds[154]. The surface of inflamed colonic mucosa is depleted of mucus but enriched with positively charged proteins; this allows for inflammatory site-specific bonding of negatively charged materials[155]. Additionally, mucus can be physically expelled by using the strong magnetic attraction between a magnetic hydrogel device and an external magnetic field to anchor a device onto the GI mucosa of living rodents for 7 days (REF.[156]).

Microrobots and nanorobots made from zinc and magnesium that self-propel in gastric and intestinal fluids can also effectively penetrate mucus to enable prolonged retention times of ~12 h in the GI tract of mice[157,158]. Compared with strategies that require the application of an external field to drive penetration, this approach benefits from autonomous locomotion driven by the local chemical environment.

Mechanical anchoring systems. Beneath the mucus layer, miniature mechanical anchoring systems enable minimally invasive device retention by gripping onto the mucosa at millimetre-scale depths (FIG. 4c). For instance, needle electrodes with hooked[159] or barbed[160] tips can achieve penetration depths of ~1 mm into the mucosa using spring-based self-injection to establish robust electrical paths into the underlying muscular layer. A snake-skin-inspired, drug-delivering stent has achieved penetration depths of up to 1 mm into the oesophageal mucosa of swine models for localized drug delivery. The in vivo and ex vivo potential of such an approach to mechanically interface with the respiratory and vascular lumen was also demonstrated[161]. However, the long-term efficacy and safety of the stent device remain to be evaluated. Another device, which was inspired by GI parasites, autonomously latched onto the mucosal tissue and remained in the GI tract of live animals for 24 h (REF.[162]). Furthermore, endoparasitic worms inspired a biphasic cone-shaped microneedle array with 700-μm-long swellable hydrogel tips that facilitated needle insertion and mechanical interlocking with both the skin and intestinal tissue[163]. The soft microneedle tips enabled device removal without damaging or inflaming the tissue. By coating the microneedle tips with mucoadhesives, retention times in the mucosa could be increased through a combination of mechanical interlocking and covalent bonding[164]. However, the long-term stability and safety of these mucosa-penetrating approaches require further evaluation.

Luminal confinement. Another strategy for long-term retention involves devices and dosage forms that can be geometrically retained within the confined lumens of the mucosa-covered organs to prevent further passage or expulsion (FIG. 4d). These forms include systems that comprise elastic recoiling components[165] or swelling hydrogels[32] that expand volumetrically once they are introduced into confined spaces such as the stomach and intestines[166] and potentially in bladders when delivered through urinary catheters. In the GI system, this approach has enabled the integration of capsule-like bulk sensors[119,167] that can achieve gastric residence of up to several months as opposed to conventional capsule electronics that transit within 24 h. Long-term retention in the female reproductive system can similarly be accomplished by leveraging well-established form factors like intrauterine devices, which are already widely used for months-long contraception. However, these systems are much stiffer than the surrounding tissues, are macroscopic, and can freely slide within enclosed mucosal cavities, and, thus, are insufficient for continuous measurements that demand a conformal sensor–tissue interface, such as electrophysiological or strain recordings.

Localization and removal

Beyond establishing a robust sensor–tissue interface with long-term retention, minimally invasive methods for delivering and localizing devices to regions of interest as well as removing devices after use are also challenging. Addressing these challenges is key to increasing the detection accuracy and minimizing the burden on patients to enable clinical translation and widespread use.

Localization. Physical access to the mucosa is more challenging than with skin and usually requires invasive procedures such as surgery or endoscopy. Ideally, MIE insertion would use non-invasive routes that are relatively routine for patients, such as ingestion (GI system) or inhalation (respiratory). Once inside the body, the ability to selectively target specific regions can increase diagnostic accuracy. For example, the digestive tract displays regional pH variations, and capsule chemistry can be readily manipulated by selecting different polymers that dissolve in either the stomach (low pH) or intestines (high pH)[168]. Enzymes with varying spatial distribution in the digestive tract have also been harnessed for targeting specific regions for device delivery. For example, catalase is present in high concentrations in the small intestine and can react with hydrogen peroxide to generate oxygen, which, in turn, initiates the polymerization of dopamine into polydopamine. Oral delivery of dopamine and hydrogen peroxide thus enables the selective deposition of synthetic epithelial linings onto the small intestine[107].

Other approaches exploit external energy fields to non-invasively navigate and trigger devices within the body. Static magnetic fields are considered safe for humans even at relatively high intensities[169] and have been exploited to manipulate microscale magnetic devices for localized drug delivery[170], biopsy[158,171] and sensing[156] in vivo. Functional nanoparticles that can circulate systemically have been used to locally activate

ion-channel-expressing, heat-sensitive neurons, mostly in deep brain regions of rodents[172,173], by converting incident magnetic or ultrasound fields into thermal energy. To position devices within the GI mucosa, an origami-inspired, magnetic-hydrogel-based ingestible device was navigated using an applied external magnetic field and deployed in specific locations on the gastric mucosa to treat gastric ulcers[174]. Near-infrared light can reach penetration depths of up to 7 cm in tissues and has been used to remotely activate gas generation from magnesium-coated, drug-loaded microdevices for controlled propulsion in GI fluids[175].

Advanced imaging technologies[175,176] have been used in parallel with the techniques described above to facilitate precise and closed-loop control during in vivo device navigation. For example, a near-infrared fluorescence-based imaging technique was developed to localize magnetic microdevices within the GI tract[177]. Microdevice localization has also been achieved using built-in addressable radio-frequency (RF) transmitters that function as magnetic spins, taking inspiration from traditional magnetic resonance imaging. These miniaturized transmitters (<0.7 mm^3) encode their spatial information by shifting their output frequency proportional to the local magnetic field during a typical magnetic resonance imaging scan with sub-millimetre resolution[178].

Removal. Removing devices from the body traditionally requires endoscopy or surgery, undermining the accessibility and acceptability of the technique. Novel strategies to remove long-term MIE without rehospitalization are therefore crucial to expand their utility beyond the clinic. For parts of the body with self-clearance functions (such as the digestive tract), materials with triggerable disintegration can be used to break down devices into smaller fragments that can be naturally cleared from the body. Endogenous triggers include physiological (for example, changes in body temperature[179], local pH[180] and enzyme concentrations[107]) and pathological (for example, the presence of inflammation markers[155] or toxins[181]) cues that originate from within the body, whereas exogenous triggers include applied heat[182], light[183], ultrasound[184] and electromagnetic fields[185,186]. For example, chemically triggerable hydrogel bioadhesives with cleavable crosslinkers can form adhesive bonds with tissues that can be subsequently detached when exposed to biocompatible chemical reagents, which could be ingested or injected at the target site[187]. Additionally, electroadhesives demonstrate reversible adhesion upon the application of an electrical field of the opposite polarity with the same magnitude[154].

An alternative approach is to construct devices made entirely from bioresorbable materials[188], which completely dissolve after a preset period, leaving only biocompatible degradation products that can be safely absorbed by the body. Retention time can be roughly tuned by selecting materials with desirable in vivo dissolution rates, which can range from several hours to multiple months, depending on both the material and its biochemical environment. The most common bioresorbable polymers rely on the hydrolysis of ester bonds, although the rate of dissolution can depend on whether degradation occurs through surface or bulk mechanisms, which can be modulated by variables such as molecular weight, crystallinity and hydrophilicity[189]. Structural and materials engineering strategies using these materials enable the fabrication of bioresorbable devices with the skin-inspired mechanical properties that are needed to form low-impedance and robust interfaces with the target tissues[189].

Communications and powering

Radio-frequency communications and power transfer. Sensor data generated from MIE need to be downloaded wirelessly in real time to maximize their diagnostic potential. RF transmission is one of the most common technologies for communicating with body-interfaced electronics[190,191], but requires on-board antennae that have dimensions of at least a quarter of the wavelength of the RF signals; the optimal size of the antenna can easily exceed several centimetres for RF signals in the sub-gigahertz range[192]. This size becomes impractical when deploying such devices through the narrow tracts that must be traversed to access the mucosa. To circumvent this issue, satellite-inspired foldable antennae[193] can be used to increase the transmission efficiency and facilitate in vivo deployment. Additionally, near-field inductive coupling[194] and ultrasound[195] techniques that exploit miniaturized antennae are being explored for communicating with electronics located 5–20 cm beneath the skin.

Batteries are generally unfavourable for body-interfacing electronics owing to their bulkiness, safety concerns and limited ability to support long-term operations. Wireless energy transfer using RF technologies has been evaluated for powering battery-less electronics interfaced with the gastric mucosa of swine, but the wireless power transfer efficiency was reduced owing to signal attenuation through tissue, limited antenna size and poorly defined antenna orientation; a power transfer efficiency of −36.1 dB was achieved using these ingestible antennae at 1.2 GHz, corresponding to a power level of 123 μW (REF.[196]). US federal regulations (such as those introduced by the Federal Communications Commission (FCC) and the International Commission on Non-Ionizing Radiation Protection (ICNIRP)) give limits on the maximum RF intensity that the human body should receive, translating to a maximum transferable power of ~150 mW in typical electronics with ingestible antennae[197]. Future efforts point towards hardware innovations such as topological optimization of the antenna configurations to enhance magnetic resonant coupling[198], as well as software advances such as beamforming algorithms that focus energy onto implanted devices[199] to enhance wireless energy transfer efficiency.

Self-powered devices. Electronics that harvest energy from endogenous and exogenous sources could address the fundamental limitations of wireless power transfer. SIE integrated with flexible and wearable energy harvesters have been developed that harvest power from exogenous sources such as light[200] and touch[201], and from endogenous sources such as body heat[202], human motion[203] and biofuels[204]. In mucosa-covered organs,

self-powered systems can be realized by harvesting mechanical energy from spontaneous organ movements or chemical energy from biofuels. Small electronic devices that can be entirely powered by GI peristalsis[205] or breathing movements[206] have been demonstrated in rodents. Biofuels rich in chemical energy, such as glucose, urea and acids, are present in large quantities in the digestive and urinary tracts; they can be converted into electricity through redox reactions using galvanic cells with the electrode pairs immersed in biofluid[207]. For example, acidic gastric fluid has been exploited as an energy source for ingestible devices using zinc and copper as electrode pairs. This mechanism yielded a peak voltage of 0.5 V and an average power density of 23 $\mu W\,cm^{-2}$ for up to 1 week in swine, which was sufficient to operate on-board temperature sensors, wireless communication modules and drug-releasing membranes[33].

Outlook and conclusion

Overall, despite the various materials and engineering challenges, there are tremendous opportunities for MIE to expand the current capacity of patient (and athlete) monitoring, diagnostics and therapeutics. We expect that the early efforts to commercialize MIE will be centred around transient acute diagnostic interventions such as motility evaluation[208].

Most existing clinical techniques used at the inner surface mucosa are minimally invasive but rely on bulky and expensive instruments (such as radiography, computerized tomography and blood panel tests), which not only limits patient throughput and increases costs but it also means that these techniques lack the ability to perform continuous, unperturbed monitoring. As technology advances, MIE may one day complement or even replace these diagnostic procedures to enable the evaluation of internal diseases in non-clinical settings, with longer measurement durations, lower costs and higher patient acceptance than present techniques.

Furthermore, with the continual development of biochemical sensors that can withstand in vivo conditions and track changes in microflora and hormones over time, MIE may offer a way to quantitatively assess several mental and neurodegenerative disorders that exhibit correlation with altered mucosal biochemical content, such as autism[209], depression[210] and Alzheimer disease[211], without the need for the transcranial placement of sensors in the brain.

MIE may also offer therapeutic opportunities that are unachievable using existing SIE. Having easy access to nerves and vasculature at or near the mucosa, MIE may provide a superior platform for closed-loop neuromodulation and therapy than that which can be achieved with SIE. Future iterations of mucosa-interfacing systems are likely to involve increased complexity in the form of novel synergies with drug delivery, which is particularly relevant for digestive MIE, as more than 90% of drugs are currently administered orally for GI mucosal absorption[212]. In general, the drug delivery field shares many major goals with MIE. For instance, regional targeting minimizes the off-target effects of active pharmaceutical ingredients[213] and long-term retention of drug delivery devices increases medication compliance[214]. Synergies with technologies that provide mechanical, optical and electrical stimulation are also expected. Therefore, there are tremendous opportunities for MIE to provide not only continuous health monitoring but also to deliver real-time therapeutic responses.

Several additional challenges need to be addressed before the commercialization of MIE can be achieved. First, to help ensure widespread acceptance of MIE in the medical community, researchers should consider potential safety pitfalls early in development. As many mucosa-lined regions of the body continuously transit material, such as digestion products (GI tract) or urine (bladder), safe device designs should avoid the disruption of these natural transitory functions, which could cause a medical emergency. Furthermore, although potentially toxic materials, which are often found in batteries and circuit components, can be shielded from the body through encapsulation, the possibility of encapsulant failure means that biologically benign materials and materials generally recognized as safe by the US Food and Drug Administration (FDA) should be used to construct these devices. Meanwhile, although research increasingly suggests that functional electronic materials such as liquid metals[215] and poly (3,4-ethylenedioxythiophene) polystyrene sulfonate[216,217] are non-toxic in various biomedical applications, future work should evaluate the biocompatibility of these materials specifically at the mucosal interface, which is consistent with regulatory guidance[218]. Furthermore, prior experience with FDA-approved systems known to safely transit through the GI tract[219] should be considered to help inform the physical dimensions of future MIE devices that interface with the digestive tract.

As this field develops, we anticipate that there will be a move towards reducing direct human input, as has been the case for SIE and other bio-integrated systems. For instance, closed-loop drug delivery systems will enable more continuous and targeted therapies, and smart systems for autonomous device deployment and removal will broaden accessibility to patient populations in regions without robust medical infrastructures[220]. Researchers should recognize that it is almost impossible to predict the full range of responses to a new technology, and intervening in the case of a medical emergency can be particularly challenging when devices are located within the body. Coupled with rigorous de-risking in the appropriate animal models, like swine models for GI devices[165], safety mechanisms that enable non-invasive external interventions to mitigate unforeseen complications should also be considered.

To establish correlations between biomedical data and the presence of disease on both personal and population levels, machine-learning-based approaches could be employed to detect highly non-linear patterns within weakly correlated data[221]. Artificial intelligence algorithms for noise detection[222] and multitasking[223,224] can also enhance the speed and quality of data processing as the total number of sensors carried by a single person continues to increase.

Published online 14 September 2022

1. Classen, C. Review of W. F. Bynum and Roy Porter, Medicine and the Five Senses. Cambridge University Press, 1993. 331 pp. *J. Hist. Behav. Sci.* **31**, 402–403 (1995).
2. Nelson, W. G., Rosen, A. & Pronovost, P. J. Reengineering the physical examination for the new millennium? *JAMA* **315**, 2391–2392 (2016).
3. Neuman, M. R. et al. Advances in medical devices and medical electronics. *Proc. IEEE* **100**, 1537–1550 (2012).
4. Xu, S., Jayaraman, A. & Rogers, J. A. Skin sensors are the future of health care. *Nature* **571**, 319–321 (2019).
5. Hammock, M. L., Chortos, A., Tee, B. C.-K., Tok, J. B.-H. & Bao, Z. 25th anniversary article: the evolution of electronic skin (e-skin): a brief history, design considerations, and recent progress. *Adv. Mater.* **25**, 5997–6038 (2013).
6. Liu, Y., Pharr, M. & Salvatore, G. A. Lab-on-skin: a review of flexible and stretchable electronics for wearable health monitoring. *ACS Nano* **11**, 9614–9635 (2017).
7. Dwivedi, A. D., Srivastava, G., Dhar, S. & Singh, R. A decentralized privacy-preserving healthcare blockchain for IoT. *Sensors* **19**, 326 (2019).
8. Ray, T. R. et al. Bio-integrated wearable systems: a comprehensive review. *Chem. Rev.* **119**, 5461–5533 (2019).
This paper provides a comprehensive review of SIE, from design and fabrication, to systematic integration with communication and powering modules, to early clinical and commercial applications.
9. Chortos, A., Liu, J. & Bao, Z. Pursuing prosthetic electronic skin. *Nat. Mater.* **15**, 937–950 (2016).
10. Wang, C., Wang, C., Huang, Z. & Xu, S. Materials and structures toward soft electronics. *Adv. Mater.* **30**, 1801368 (2018).
11. Xu, C., Yang, Y. & Gao, W. Skin-interfaced sensors in digital medicine: from materials to applications. *Matter* **2**, 1414–1445 (2020).
12. Liu, J., Bian, Z., Kuijpers-Jagtman, A. M. & Von den Hoff, J. W. Skin and oral mucosa equivalents: construction and performance. *Orthod. Craniofac. Res.* **13**, 11–20 (2010).
13. Steiger, C. et al. Ingestible electronics for diagnostics and therapy. *Nat. Rev. Mater.* **4**, 83–98 (2019).
Focusing on ingestible electronics, this review provides a detailed overview of several of the challenges associated with deploying and operating devices within the GI tract, including communication and powering.
14. Kissler, K. J., Lowe, N. K. & Hernandez, T. L. An integrated review of uterine activity monitoring for evaluating labor dystocia. *J. Midwifery Womens Health* **65**, 323–334 (2020).
15. Sang, L. et al. A narrative review of electrical impedance tomography in lung diseases with flow limitation and hyperinflation: methodologies and applications. *Ann. Transl. Med.* **8**, 1688 (2020).
16. Angeli, T. R., O'Grady, G., Vather, R., Bissett, I. P. & Cheng, L. K. Intra-operative high-resolution mapping of slow wave propagation in the human jejunum: feasibility and initial results. *Neurogastroenterol. Motil.* **30**, e13310 (2018).
17. Cherian Abraham, A., Cheng, L. K., Angeli, T. R., Alighaleh, S. & Paskaranandavadivel, N. Dynamic slow-wave interactions in the rabbit small intestine defined using high-resolution mapping. *Neurogastroenterol. Motil.* **31**, e13670 (2019).
18. LaPallo, B. K., Wolpaw, J. R., Chen, X. Y. & Carp, J. S. Long-term recording of external urethral sphincter EMG activity in unanesthetized, unrestrained rats. *Am. J. Physiol. Renal Physiol.* **307**, F485–F497 (2014).
19. O'Grady, G. et al. Abnormal initiation and conduction of slow-wave activity in gastroparesis, defined by high-resolution electrical mapping. *Gastroenterology* **143**, 589–598.e3 (2012).
20. Pandolfino, J. E. et al. Comparison of the Bravo wireless and Digitrapper catheter-based pH monitoring systems for measuring esophageal acid exposure. *Am. J. Gastroenterol.* **100**, 1466–1476 (2005).
21. Bigelow, J. L. Mucus observations in the fertile window: a better predictor of conception than timing of intercourse. *Hum. Reprod.* **19**, 889–892 (2004).
22. Gonzalez-Guillaumin, J. L., Sadowski, D. C., Kaler, K. V. I. S. & Mintchev, M. P. Ingestible capsule for impedance and pH monitoring in the esophagus. *IEEE Trans. Biomed. Eng.* **54**, 2231–2236 (2007).
23. Sommer, F. & Bäckhed, F. The gut microbiota — masters of host development and physiology. *Nat. Rev. Microbiol.* **11**, 227–238 (2013).
24. Fan, Y. & Pedersen, O. Gut microbiota in human metabolic health and disease. *Nat. Rev. Microbiol.* **19**, 55–71 (2021).
This review discusses the coupling between gut microbiota and the metabolism of healthy and diseased hosts, as well as microbiota-targeted interventions that aim to optimize metabolic health.
25. Chakraborty, A., Dasari, S., Long, W. & Mohan, C. Urine protein biomarkers for the detection, surveillance, and treatment response prediction of bladder cancer. *Am. J. Cancer Res.* **9**, 1104–1117 (2019).
This paper identifies several urinary biomarkers that may facilitate the detection, surveillance and monitoring of bladder cancer, serving as potential target analytes when developing mucosa-interfaced biosensors in the urinary tract.
26. Grande, G. et al. Cervical mucus proteome in endometriosis. *Clin. Proteom.* **14**, 7 (2017).
27. Shen, C.-J. et al. Clinical evaluation of a self-testing kit for vaginal infection diagnosis. *J. Healthc. Eng.* **2021**, 4948954 (2021).
28. Zimmermann, C. J. & Lidor, A. Endoscopic and surgical management of gastroesophageal reflux disease. *Gastroenterol. Clin. N. Am.* **50**, 809–823 (2021).
29. Kalantar-Zadeh, K. et al. A human pilot trial of ingestible electronic capsules capable of sensing different gases in the gut. *Nat. Electron.* **1**, 79–87 (2018).
Ingestible sensors have already made remarkable progress towards clinical translation, including this human pilot trial using an ingestible gas-sensing capsule device.
30. Hutchison, J. S. et al. Hypothermia therapy after traumatic brain injury in children. *N. Engl. J. Med.* **358**, 2447–2456 (2008).
31. Sauvé, C. C., Van de Walle, J., Hammill, M. O., Arnould, J. P. Y. & Beauplet, G. Stomach temperature records reveal nursing behaviour and transition to solid food consumption in an unweaned mammal, the harbour seal pup (*Phoca vitulina*). *PLoS ONE* **9**, e90329 (2014).
32. Liu, X. et al. Ingestible hydrogel device. *Nat. Commun.* **10**, 493 (2019).
33. Nadeau, P. et al. Prolonged energy harvesting for ingestible devices. *Nat. Biomed. Eng.* **1**, 0022 (2017).
34. Cox, E. G. M. et al. Temporal artery temperature measurements versus bladder temperature in critically ill patients, a prospective observational study. *PLoS ONE* **15**, e0241846 (2020).
35. Ng, K. Y. B., Mingels, R., Morgan, H., Macklon, N. & Cheong, Y. In vivo oxygen, temperature and pH dynamics in the female reproductive tract and their importance in human conception: a systematic review. *Hum. Reprod. Update* **24**, 15–34 (2018).
36. Regidor, P.-A., Kaczmarczyk, M., Schiweck, E., Goeckenjan-Festag, M. & Alexander, H. Identification and prediction of the fertile window with a new web-based medical device using a vaginal biosensor for measuring the circadian and circamensual core body temperature. *Gynecol. Endocrinol.* **34**, 256–260 (2018).
37. Fallis, W. M. Monitoring urinary bladder temperature in the intensive care unit: state of the science. *Am. J. Crit. Care* **11**, 38–45 (2002).
38. Chung, S. C. S., Sung, J. Y., Suen, M. W. M., Leung, J. W. C. & Leung, F. W. Endoscopic assessment of mucosal hemodynamic changes in a canine model of gastric ulcer. *Gastrointest. Endosc.* **37**, 310–314 (1991).
39. Kamada, T. et al. Gastric mucosal blood distribution and its changes in the healing process of gastric ulcer. *Gastroenterology* **84**, 1541–1546 (1983).
40. Clark, A. & Tawhai, M. Pulmonary vascular dynamics. *Compr. Physiol.* **9**, 1081–1100 (2019).
41. Andersson, K.-E., Boedtkjer, D. B. & Forman, A. The link between vascular dysfunction, bladder ischemia, and aging bladder dysfunction. *Ther. Adv. Urol.* **9**, 11–27 (2017).
42. Wehrenberg, W. B., Chaichareon, D. P., Dierschke, D. J., Rankin, J. H. & Ginther, O. J. Vascular dynamics of the reproductive tract in the female rhesus monkey: relative contributions of ovarian and uterine arteries. *Biol. Reprod.* **17**, 148–153 (1977).
43. Friedland, S., Soetikno, R. & Benaron, D. Reflectance spectrophotometry for the assessment of mucosal perfusion in the gastrointestinal tract. *Gastrointest. Endosc. Clin. N. Am.* **14**, 539–553 (2004).
44. Medford, A. R. L. Endobronchial ultrasound: what is it and when should it be used? *Clin. Med.* **10**, 458–463 (2010).
45. Herth, F. J. F. in *Endobronchial Ultrasound* (eds Herth, F. J. F. & Ernst, A.) 89–101 (Springer, 2009).
46. Schweiger, C., Cohen, A. P. & Rutter, M. J. Tracheal and bronchial stenoses and other obstructive conditions. *J. Thorac. Dis.* **8**, 3369–3378 (2016).
47. Kloetzer, L. et al. Motility of the antroduodenum in healthy and gastroparetics characterized by wireless motility capsule. *Neurogastroenterol. Motil.* **22**, 527-e117 (2010).
48. Rao, S. S. C. et al. Investigation of colonic and whole-gut transit with wireless motility capsule and radiopaque markers in constipation. *Clin. Gastroenterol. Hepatol.* **7**, 537–544 (2009).
49. Artibani, W. Diagnosis and significance of idiopathic overactive bladder. *Urology* **50**, 25–32; discussion 33–5 (1997) .
50. Egorov, V. et al. Quantitative assessment and interpretation of vaginal conditions. *Sex. Med.* **6**, 39–48 (2018).
51. Zafar, M. A. et al. Manometry optimized positive expiratory pressure (MOPEP) in excessive dynamic airway collapse (EDAC). *Respir. Med.* **131**, 179–183 (2017).
52. Basu, A. S. et al. Is submucosal bladder pressure monitoring feasible? *Proc. Inst. Mech. Eng. H* **233**, 100–113 (2019).
53. Deptuła, P. et al. Nanomechanical hallmarks of *Helicobacter pylori* infection in pediatric patients. *Int. J. Mol. Sci.* **22**, 5624 (2021).
54. Esaki, M. et al. Endoscopic ultrasound elastography as a novel diagnostic method for the assessment of hardness and depth of invasion in colorectal neoplasms. *Digestion* **102**, 701–713 (2021).
55. Eskandari, M., Arvayo, A. L. & Levenston, M. E. Mechanical properties of the airway tree: heterogeneous and anisotropic pseudoelastic and viscoelastic tissue responses. *J. Appl. Physiol.* **125**, 878–888 (2018).
56. Raub, C. B. et al. Linking optics and mechanics in an in vivo model of airway fibrosis and epithelial injury. *J. Biomed. Opt.* **15**, 015004 (2010).
57. Barnes, R. W., Theodore Bergman, R. & Hadley, H. L. in *Endoscopy* Vol. 6, 85–93 (Springer, 1959).
58. Zhou, L. et al. Biomechanical properties and associated collagen composition in vaginal tissue of women with pelvic organ prolapse. *J. Urol.* **188**, 875–880 (2012).
59. White, C. B., Zimmern, P. & Eberhart, R. Vaginal biomechanics analyzer. US Patent 9730630B2 (2015).
60. de Jong, P. A. et al. Progression of lung disease on computed tomography and pulmonary function tests in children and adults with cystic fibrosis. *Thorax* **61**, 80–85 (2006).
61. Karargyris, A. & Koulaouzidis, A. OdoCapsule: next-generation wireless capsule endoscopy with accurate lesion localization and video stabilization capabilities. *IEEE Trans. Biomed. Eng.* **62**, 352–360 (2015).
62. Barbara, D. W. et al. Periprocedural management of 172 gastrointestinal endoscopies in patients with left ventricular assist devices. *ASAIO J.* **61**, 670–675 (2015).
63. Brady, J. E., Giglio, R., Keyes, K. M., DiMaggio, C. & Li, G. Risk markers for fatal and non-fatal prescription drug overdose: a meta-analysis. *Inj. Epidemiol.* **4**, 24 (2017).
64. Kusters, J. G., van Vliet, A. H. M. & Kuipers, E. J. Pathogenesis of *Helicobacter pylori* infection. *Clin. Microbiol. Rev.* **19**, 449–490 (2006).
65. Weiss, J. W. Sexually transmitted diseases of mucous membranes. *Clin. Dermatol.* **5**, 103–111 (1987).
66. Li, Y., Li, N., De Oliveira, N. & Wang, S. Implantable bioelectronics toward long-term stability and sustainability. *Matter* **4**, 1125–1141 (2021).
67. Wang, S., Oh, J. Y., Xu, J., Tran, H. & Bao, Z. Skin-inspired electronics: an emerging paradigm. *Acc. Chem. Res.* **51**, 1033–1045 (2018).
Mucosa-interfaced electronics can learn much from another comprehensive review that details materials and design approaches to achieve reliable sensor–tissue interfaces with soft and dynamic bodily surfaces for high signal fidelity.
68. Shahriari, D., Rosenfeld, D. & Anikeeva, P. Emerging frontier of peripheral nerve and organ interfaces. *Neuron* **108**, 270–285 (2020).
A perspective on design considerations and recent technological advances for bioelectronics that interface with various organs across the human body for electrical neuromodulation.

69. Egorov, V. I., Schastlivtsev, I. V., Prut, E. V., Baranov, A. O. & Turusov, R. A. Mechanical properties of the human gastrointestinal tract. *J. Biomech.* **35**, 1417–1425 (2002).
70. Xu, S. et al. Stretchable batteries with self-similar serpentine interconnects and integrated wireless recharging systems. *Nat. Commun.* **4**, 1543 (2013).
71. Xu, S. et al. Soft microfluidic assemblies of sensors, circuits, and radios for the skin. *Science* **344**, 70–74 (2014).
72. Yang, X. et al. Bioinspired neuron-like electronics. *Nat. Mater.* **18**, 510–517 (2019).
One of the softest sensors created to date, this work presents a method to build neuron-like sensor–tissue interfaces for three-dimensional electrophysiological mapping in living rodents.
73. Hong, G. et al. A method for single-neuron chronic recording from the retina in awake mice. *Science* **360**, 1447–1451 (2018).
74. Zhao, L. et al. Highly-stable polymer-crosslinked 2D MXene-based flexible biocompatible electronic skins for in vivo biomonitoring. *Nano Energy* **84**, 105921 (2021).
75. Dagdeviren, C. et al. Flexible piezoelectric devices for gastrointestinal motility sensing. *Nat. Biomed. Eng.* **1**, 807–817 (2017).
76. Someya, T. & Wang, S. in *Stretchable Electronics* (ed. Someya, T.) 1–29 (Wiley, 2012).
77. Mickle, A. D. et al. A wireless closed-loop system for optogenetic peripheral neuromodulation. *Nature* **565**, 361–365 (2019).
This paper is one of the first demonstrations of closed-loop therapy enabled by real-time physiological (strain) data collected from urinary mucosa of living rodents.
78. Dejace, L., Chen, H., Furfaro, I., Schiavone, G. & Lacour, S. P. Microscale liquid metal conductors for stretchable and transparent electronics. *Adv. Mater. Technol.* **6**, 2100690 (2021).
79. Yeo, W.-H. et al. Multifunctional epidermal electronics printed directly onto the skin. *Adv. Mater.* **25**, 2773–2778 (2013).
80. Kaltenbrunner, M. et al. An ultra-lightweight design for imperceptible plastic electronics. *Nature* **499**, 458–463 (2013).
81. Sun, Y., Choi, W. M., Jiang, H., Huang, Y. Y. & Rogers, J. A. Controlled buckling of semiconductor nanoribbons for stretchable electronics. *Nat. Nanotechnol.* **1**, 201–207 (2006).
82. Jang, K.-I. et al. Self-assembled three dimensional network designs for soft electronics. *Nat. Commun.* **8**, 15894 (2017).
83. Blees, M. K. et al. Graphene kirigami. *Nature* **524**, 204–207 (2015).
84. Luo, Y. et al. Learning human–environment interactions using conformal tactile textiles. *Nat. Electron.* **4**, 193–201 (2021).
85. Balint, R., Cassidy, N. J. & Cartmell, S. H. Conductive polymers: towards a smart biomaterial for tissue engineering. *Acta Biomater.* **10**, 2341–2353 (2014).
86. Dickey, M. D. Stretchable and soft electronics using liquid metals. *Adv. Mater.* **29**, 1606425 (2017).
87. Matsuhisa, N. et al. Printable elastic conductors by in situ formation of silver nanoparticles from silver flakes. *Nat. Mater.* **16**, 834–840 (2017).
88. Xu, J. et al. Highly stretchable polymer semiconductor films through the nanoconfinement effect. *Science* **355**, 59–64 (2017).
89. Wang, S. et al. Skin electronics from scalable fabrication of an intrinsically stretchable transistor array. *Nature* **555**, 83–88 (2018).
90. Tringides, C. M. et al. Viscoelastic surface electrode arrays to interface with viscoelastic tissues. *Nat. Nanotechnol.* **16**, 1019–1029 (2021).
91. Liu, Y. et al. Morphing electronics enable neuromodulation in growing tissue. *Nat. Biotechnol.* **38**, 1031–1036 (2020).
92. Li, J. et al. A tissue-like neurotransmitter sensor for the brain and gut. *Nature* **606**, 94–101 (2022).
This paper is one of the earliest demonstrations of mucosa-interfacing biochemical sensor arrays for real-time assessment of the brain–gut axis in living rodents.
93. Liu, Y. et al. Soft and elastic hydrogel-based microelectronics for localized low-voltage neuromodulation. *Nat. Biomed. Eng.* **3**, 58–68 (2019).
94. Ying, B., Chen, R. Z., Zuo, R., Li, J. & Liu, X. An anti-freezing, ambient-stable and highly stretchable ionic skin with strong surface adhesion for wearable sensing and soft robotics. *Adv. Funct. Mater.* **31**, 2104665 (2021).
95. Yang, Q., Hu, Z. & Rogers, J. A. Functional hydrogel interface materials for advanced bioelectronic devices. *Acc. Mater. Res.* **2**, 1010–1023 (2021).
96. Yuk, H., Lu, B. & Zhao, X. Hydrogel bioelectronics. *Chem. Soc. Rev.* **48**, 1642–1667 (2019).
97. Oribe, S. et al. Hydrogel-based organic subdural electrode with high conformability to brain surface. *Sci. Rep.* **9**, 13379 (2019).
98. Alizadeh-Meghrazi, M. et al. Evaluation of dry textile electrodes for long-term electrocardiographic monitoring. *Biomed. Eng. Online* **20**, 68 (2021).
99. Yang, Q. et al. Photocurable bioresorbable adhesives as functional interfaces between flexible bioelectronic devices and soft biological tissues. *Nat. Mater.* **20**, 1559–1570 (2021).
100. Deng, J. et al. Electrical bioadhesive interface for bioelectronics. *Nat. Mater.* **20**, 229–236 (2021).
This work is one of the first demonstrations of sensor–tissue interfaces using hydrogels that simultaneously enhance signal fidelity and improve device retention on the tissue surface.
101. Yuk, H. et al. Dry double-sided tape for adhesion of wet tissues and devices. *Nature* **575**, 169–174 (2019).
102. Li, J. et al. Tough adhesives for diverse wet surfaces. *Science* **357**, 378–381 (2017).
103. Wu, S. J., Yuk, H., Wu, J., Nabzdyk, C. S. & Zhao, X. A multifunctional origami patch for minimally invasive tissue sealing. *Adv. Mater.* **33**, e2007667 (2021).
104. Wu, J. et al. An off-the-shelf bioadhesive patch for sutureless repair of gastrointestinal defects. *Sci. Transl. Med.* **14**, abh2857 (2022).
105. Sender, R. & Milo, R. The distribution of cellular turnover in the human body. *Nat. Med.* **27**, 45–48 (2021).
A study examining cellular turnover rates, these results are critical, as turnover poses a major challenge for long-term retention and operability of mucosa-interfaced devices.
106. Lee, Y.-A. L., Zhang, S., Lin, J., Langer, R. & Traverso, G. A Janus mucoadhesive and omniphobic device for gastrointestinal retention. *Adv. Healthc. Mater.* **5**, 1141–1146 (2016).
107. Li, J. et al. Gastrointestinal synthetic epithelial linings. *Sci. Transl. Med.* **12**, eabc0441 (2020).
This example of an in situ-forming mucosa-interfacing material could inspire future methods for targeting and localizing mucosa-interfacing sensors to specific regions of the body.
108. Koo, H. et al. Bioorthogonal copper-free click chemistry in vivo for tumor-targeted delivery of nanoparticles. *Angew. Chem. Int. Ed.* **124**, 12006–12010 (2012).
109. Liu, J. et al. Genetically targeted chemical assembly of functional materials in living cells, tissues, and animals. *Science* **367**, 1372–1376 (2020).
110. Li, B. et al. De novo design of functional zwitterionic biomimetic material for immunomodulation. *Sci. Adv.* **6**, eaba0754 (2020).
111. Zhang, L. et al. Zwitterionic hydrogels implanted in mice resist the foreign-body reaction. *Nat. Biotechnol.* **31**, 553–556 (2013).
112. Zhang, J. et al. Antibacterial and antifouling hybrid ionic–covalent hydrogels with tunable mechanical properties. *ACS Appl. Mater. Interfaces* **11**, 31594–31604 (2019).
113. Yuk, H., Zhang, T., Parada, G. A., Liu, X. & Zhao, X. Skin-inspired hydrogel–elastomer hybrids with robust interfaces and functional microstructures. *Nat. Commun.* **7**, 12028 (2016).
114. Wu, F., Pang, Y. & Liu, J. Swelling-strengthening hydrogels by embedding with deformable nanobarriers. *Nat. Commun.* **11**, 4502 (2020).
115. Inoue, A., Yuk, H., Lu, B. & Zhao, X. Strong adhesion of wet conducting polymers on diverse substrates. *Sci. Adv.* **6**, eaay5394 (2020).
116. Koh, A. et al. A soft, wearable microfluidic device for the capture, storage, and colorimetric sensing of sweat. *Sci. Transl. Med.* **8**, 366ra165 (2016).
117. Nyein, H. Y. Y. et al. A wearable patch for continuous analysis of thermoregulatory sweat at rest. *Nat. Commun.* **12**, 1823 (2021).
118. Reeder, J. T. et al. Waterproof, electronics-enabled, epidermal microfluidic devices for sweat collection, biomarker analysis, and thermography in aquatic settings. *Sci. Adv.* **5**, eaau6356 (2019).
119. Mimee, M. et al. An ingestible bacterial-electronic system to monitor gastrointestinal health. *Science* **360**, 915–918 (2018).
This work is one of the first demonstrations of gut-interfacing bacteria sensors that can identify gastric bleeding in real time, pushing the boundary of sensor designs beyond conventional inorganic and organic materials to include living substances.
120. Kalantar-Zadeh, K., Ha, N., Ou, J. Z. & Berean, K. J. Ingestible sensors. *ACS Sens.* **2**, 468–483 (2017).
121. Triantafyllou, K., Chang, C. & Pimentel, M. Methanogens, methane and gastrointestinal motility. *J. Neurogastroenterol. Motil.* **20**, 31–40 (2014).
122. Otte, J. A., Geelkerken, R. H., Huisman, A. B. & Kolkman, J. J. What is the best diagnostic approach for chronic gastrointestinal ischemia? *Am. J. Gastroenterol.* **102**, 2005–2010 (2007).
123. Saylan, Y., Akgönüllü, S., Yavuz, H., Ünal, S. & Denizli, A. Molecularly imprinted polymer based sensors for medical applications. *Sensors* **19**, 1279 (2019).
124. Parlak, O., Keene, S. T., Marais, A., Curto, V. F. & Salleo, A. Molecularly selective nanoporous membrane-based wearable organic electrochemical device for noninvasive cortisol sensing. *Sci. Adv.* **4**, eaar2904 (2018).
125. Song, E., Li, J., Won, S. M., Bai, W. & Rogers, J. A. Materials for flexible bioelectronic systems as chronic neural interfaces. *Nat. Mater.* **19**, 590–603 (2020).
126. Wong, T.-S. et al. Bioinspired self-repairing slippery surfaces with pressure-stable omniphobicity. *Nature* **477**, 443–447 (2011).
127. Sun, H. et al. Bioinspired oil-infused slippery surfaces with water and ion barrier properties. *ACS Appl. Mater. Interfaces* **13**, 33464–33476 (2021).
128. Johannessen, E. A., Wang, L., Wyse, C., Cumming, D. R. S. & Cooper, J. M. Biocompatibility of a lab-on-a-pill sensor in artificial gastrointestinal environments. *IEEE Trans. Biomed. Eng.* **53**, 2333–2340 (2006).
129. Chan, D. et al. Combinatorial polyacrylamide hydrogels for preventing biofouling on implantable biosensors. *Adv. Mater.* **34**, 2109764 (2022).
130. Altreuter, D. H. et al. Changing the pill: developments toward the promise of an ultra-long-acting gastroretentive dosage form. *Expert Opin. Drug Deliv.* **15**, 1189–1198 (2018).
131. Cook, M. T. & Khutoryanskiy, V. V. Mucoadhesion and mucosa-mimetic materials — A mini-review. *Int. J. Pharm.* **495**, 991–998 (2015).
132. Zhao, P. et al. Nanoparticle-assembled bioadhesive coacervate coating with prolonged gastrointestinal retention for inflammatory bowel disease therapy. *Nat. Commun.* **12**, 7162 (2021).
133. Chaturvedi, M., Kumar, M. & Pathak, K. A review on mucoadhesive polymer used in nasal drug delivery system. *J. Adv. Pharm. Technol. Res.* **2**, 215–222 (2011).
134. Rossi, S. et al. Recent advances in the mucus-interacting approach for vaginal drug delivery: from mucoadhesive to mucus-penetrating nanoparticles. *Expert Opin. Drug Deliv.* **16**, 777–781 (2019).
135. Nair, M. K. & Chien, Y. W. Development of anticandidal delivery systems: (II) mucoadhesive devices for prolonged drug delivery in the oral cavity. *Drug Dev. Ind. Pharm.* **22**, 243–253 (1996).
136. Alopaeus, J. F. et al. Mucoadhesive buccal films based on a graft co-polymer - A mucin-retentive hydrogel scaffold. *Eur. J. Pharm. Sci.* **142**, 105142 (2020).
137. Gupta, V. et al. Delivery of exenatide and insulin using mucoadhesive intestinal devices. *Ann. Biomed. Eng.* **44**, 1993–2007 (2016).
138. Banerjee, A., Lee, J. & Mitragotri, S. Intestinal mucoadhesive devices for oral delivery of insulin. *Bioeng. Transl. Med.* **1**, 338–346 (2016).
139. Han, K. et al. Generation of systemic antitumour immunity via the in situ modulation of the gut microbiome by an orally administered inulin gel. *Nat. Biomed. Eng.* **5**, 1377–1388 (2021).
140. Cao, Y. & Mezzenga, R. Design principles of food gels. *Nat. Food* **1**, 106–118 (2020).
141. Leal, J., Smyth, H. D. C. & Ghosh, D. Physicochemical properties of mucus and their impact on transmucosal drug delivery. *Int. J. Pharm.* **532**, 555–572 (2017).
142. Maisel, K., Ensign, L., Reddy, M., Cone, R. & Hanes, J. Effect of surface chemistry on nanoparticle interaction with gastrointestinal mucus and distribution in the gastrointestinal tract following oral and rectal administration in the mouse. *J. Control. Release* **197**, 48–57 (2015).
143. Popov, A. Mucus-penetrating particles and the role of ocular mucus as a barrier to micro- and nanosuspensions. *J. Ocul. Pharmacol. Ther.* **36**, 366–375 (2020).
144. Mathiowitz, E. et al. Biologically erodable microspheres as potential oral drug delivery systems. *Nature* **386**, 410–414 (1997).

145. Ensign, L. M. et al. Mucus-penetrating nanoparticles for vaginal drug delivery protect against herpes simplex virus. *Sci. Transl. Med.* **4**, 138ra79 (2012).
146. Baik, S. et al. Bioinspired adhesive architectures: from skin patch to integrated bioelectronics. *Adv. Mater.* **31**, e1803309 (2019).
147. Cheung, E., Karagozler, M. E., Park, S., Kim, B. & Sitti, M. in *Proc. 2005 IEEE/ASME Int. Conf. Adv. Intell. Mechatron.* https://doi.org/10.1109/aim.2005.1511040 (IEEE, 2015).
148. Baik, S. et al. A wet-tolerant adhesive patch inspired by protuberances in suction cups of octopi. *Nature* **546**, 396–400 (2017).
149. Lee, H., Lee, B. P. & Messersmith, P. B. A reversible wet/dry adhesive inspired by mussels and geckos. *Nature* **448**, 338–341 (2007).
150. Mahdavi, A. et al. A biodegradable and biocompatible gecko-inspired tissue adhesive. *Proc. Natl Acad. Sci. USA* **105**, 2307–2312 (2008).
151. Wang, S. et al. in *Proc. 2019 Int. Conf. Robot. Autom. (ICRA)* https://doi.org/10.1109/icra.2019.8793703 (IEEE, 2019).
152. Nishikawa, M., Hasegawa, S., Yamashita, F., Takakura, Y. & Hashida, M. Electrical charge on protein regulates its absorption from the rat small intestine. *Am. J. Physiol. Gastrointest. Liver Physiol.* **282**, G711–G719 (2002).
153. Bansil, R. & Turner, B. S. The biology of mucus: composition, synthesis and organization. *Adv. Drug Deliv. Rev.* **124**, 3–15 (2018).
154. Borden, L. K., Gargava, A. & Raghavan, S. R. Reversible electroadhesion of hydrogels to animal tissues for suture-less repair of cuts or tears. *Nat. Commun.* **12**, 4419 (2021).
155. Zhang, S. et al. An inflammation-targeting hydrogel for local drug delivery in inflammatory bowel disease. *Sci. Transl. Med.* **7**, 300ra128 (2015).
156. Liu, X. et al. Magnetic living hydrogels for intestinal localization, retention, and diagnosis. *Adv. Funct. Mater.* **31**, 2010918 (2021).
A demonstration of the localization and retention of a device using magnetic materials and an external magnetic field.
157. de Ávila, B. E.-F. et al. Micromotor-enabled active drug delivery for in vivo treatment of stomach infection. *Nat. Commun.* **8**, 272 (2017).
158. Li, J., Esteban-Fernández de Ávila, B., Gao, W., Zhang, L. & Wang, J. Micro/nanorobots for biomedicine: delivery, surgery, sensing, and detoxification. *Sci. Robot.* **2**, eaam6431 (2017).
159. Abramson, A. et al. Ingestible transiently anchoring electronics for microstimulation and conductive signaling. *Sci. Adv.* **6**, eaaz0127 (2020).
This work demonstrates a non-invasive oral delivery mechanism to introduce an electronic device capable of interfacing with the mucosal surface.
160. Liu, S., Chu, S., Banis, G. E., Beardslee, L. A. & Ghodssi, R. in *Proc. 2020 IEEE 33rd Int. Conf. Micro Electro Mech. Syst. (MEMS)* https://doi.org/10.1109/mems46641.2020.9056127 (IEEE, 2020).
161. Babaee, S. et al. Kirigami-inspired stents for sustained local delivery of therapeutics. *Nat. Mater.* **20**, 1085–1092 (2021).
162. Ghosh, A. et al. Gastrointestinal-resident, shape-changing microdevices extend drug release in vivo. *Sci. Adv.* **6**, eabb4133 (2020).
163. Yang, S. Y. et al. A bio-inspired swellable microneedle adhesive for mechanical interlocking with tissue. *Nat. Commun.* **4**, 1702 (2013).
164. Zhao, X. et al. Soft materials by design: unconventional polymer networks give extreme properties. *Chem. Rev.* **121**, 4309–4372 (2021).
165. Bellinger, A. M. et al. Oral, ultra–long-lasting drug delivery: application toward malaria elimination goals. *Sci. Transl. Med.* **8**, 365ra157 (2016).
166. Abramson, A. et al. A luminal unfolding microneedle injector for oral delivery of macromolecules. *Nat. Med.* **25**, 1512–1518 (2019).
167. Kong, Y. L. et al. 3D-printed gastric resident electronics. *Adv. Mater. Technol.* **4**, 1800490 (2019).
168. Hua, S. Advances in oral drug delivery for regional targeting in the gastrointestinal tract-influence of physiological, pathophysiological and pharmaceutical factors. *Front. Pharmacol.* **11**, 524 (2020).
169. Shellock, F. G., Schaefer, D. J. & Gordon, C. J. Effect of a 1.5 T static magnetic field on body temperature of man. *Magn. Reson. Med.* **3**, 644–647 (1986).
170. Zhang, X., Chen, G., Fu, X., Wang, Y. & Zhao, Y. Magneto-responsive microneedle robots for intestinal macromolecule delivery. *Adv. Mater.* **33**, e2104932 (2021).
171. Ghosh, A., Liu, Y., Artemov, D. & Gracias, D. H. Magnetic resonance guided navigation of untethered microgrippers. *Adv. Healthc. Mater.* **10**, e2000869 (2021).
172. Chen, R., Romero, G., Christiansen, M. G., Mohr, A. & Anikeeva, P. Wireless magnetothermal deep brain stimulation. *Science* **347**, 1477–1480 (2015).
173. Wu, X. et al. Tether-free photothermal deep-brain stimulation in freely behaving mice via wide-field illumination in the near-infrared-II window. *Nat. Biomed. Eng.* **6**, 754–770 (2022).
174. d'Argentre, A. et al. in *Proc. 2018 IEEE Int. Conf. Robot. Autom. (ICRA)* https://doi.org/10.1109/icra.2018.8460615 (IEEE, 2018).
175. Wu, Z. et al. A microrobotic system guided by photoacoustic computed tomography for targeted navigation in intestines in vivo. *Sci. Robot.* **4**, eaax0613 (2019).
176. Yan, X. et al. Multifunctional biohybrid magnetite microrobots for imaging-guided therapy. *Sci. Robot.* **2**, eaaq1155 (2017).
177. Servant, A., Qiu, F., Mazza, M., Kostarelos, K. & Nelson, B. J. Controlled in vivo swimming of a swarm of bacteria-like microrobotic flagella. *Adv. Mater.* **27**, 2981–2988 (2015).
178. Monge, M., Lee-Gosselin, A., Shapiro, M. G. & Emami, A. Localization of microscale devices in vivo using addressable transmitters operated as magnetic spins. *Nat. Biomed. Eng.* **1**, 736–744 (2017).
179. Babaee, S. et al. Temperature-responsive biometamaterials for gastrointestinal applications. *Sci. Transl. Med.* **11**, eaau8581 (2019).
180. Nejad, H. R. et al. Ingestible osmotic pill for in vivo sampling of gut microbiomes. *Adv. Intell. Syst.* **1**, 1970052 (2019).
181. Pornpattananangkul, D. et al. Bacterial toxin-triggered drug release from gold nanoparticle-stabilized liposomes for the treatment of bacterial infection. *J. Am. Chem. Soc.* **133**, 4132–4139 (2011).
182. Verma, M. et al. A gastric resident drug delivery system for prolonged gram-level dosing of tuberculosis treatment. *Sci. Transl. Med.* **11**, eaau6267 (2019).
183. Raman, R. et al. Light-degradable hydrogels as dynamic triggers for gastrointestinal applications. *Sci. Adv.* **6**, eaay0065 (2020).
184. Sun, T., Dasgupta, A., Zhao, Z., Nurunnabi, M. & Mitragotri, S. Physical triggering strategies for drug delivery. *Adv. Drug Deliv. Rev.* **158**, 36–62 (2020).
185. Koo, J. et al. Wirelessly controlled, bioresorbable drug delivery device with active valves that exploit electrochemically triggered crevice corrosion. *Sci. Adv.* **6**, eabb1093 (2020).
186. Thévenot, J., Oliveira, H., Sandre, O. & Lecommandoux, S. Magnetic responsive polymer composite materials. *Chem. Soc. Rev.* **42**, 7099–7116 (2013).
187. Chen, X., Yuk, H., Wu, J., Nabzdyk, C. S. & Zhao, X. Instant tough bioadhesive with triggerable benign detachment. *Proc. Natl Acad. Sci. USA* **117**, 15497–15503 (2020).
188. Hwang, S.-W. et al. A physically transient form of silicon electronics. *Science* **337**, 1640–1644 (2012).
This work provides an example of how bioresorbable materials may be used to construct bioelectronic devices that do not need to be removed with an invasive procedure when the device is at the end of its life cycle.
189. Feig, V. R., Tran, H. & Bao, Z. Biodegradable polymeric materials in degradable electronic devices. *ACS Cent. Sci.* **4**, 337–348 (2018).
190. Chung, H. U. et al. Binodal, wireless epidermal electronic systems with in-sensor analytics for neonatal intensive care. *Science* **363**, eaau0780 (2019).
191. Chung, H. U. et al. Skin-interfaced biosensors for advanced wireless physiological monitoring in neonatal and pediatric intensive-care units. *Nat. Med.* **26**, 418–429 (2020).
192. Poon, A. S. Y., O'Driscoll, S. & Meng, T. H. Optimal frequency for wireless power transmission into dispersive tissue. *IEEE Trans. Antennas Propag.* **58**, 1739–1750 (2010).
193. Zhou, N., Liu, C., Lewis, J. A. & Ham, D. Gigahertz electromagnetic structures via direct ink writing for radio-frequency oscillator and transmitter applications. *Adv. Mater.* **29**, 1605198 (2017).
194. Hafezi, H. et al. An ingestible sensor for measuring medication adherence. *IEEE Trans. Biomed. Eng.* **62**, 99–109 (2015).
195. Seo, D. et al. Wireless recording in the peripheral nervous system with ultrasonic neural dust. *Neuron* **91**, 529–539 (2016).
196. Abid, A. et al. Wireless power transfer to millimeter-sized gastrointestinal electronics validated in a swine model. *Sci. Rep.* **7**, 46745 (2017).
197. Lenaerts, B. & Puers, R. An inductive power link for a wireless endoscope. *Biosens. Bioelectron.* **22**, 1390–1395 (2007).
198. Gutruf, P. et al. Fully implantable optoelectronic systems for battery-free, multimodal operation in neuroscience research. *Nat. Electron.* **1**, 652–660 (2018).
199. Ma, Y., Luo, Z., Steiger, C., Traverso, G. & Adib, F. in *Proc. SOGCOMM '18: 2018 Conf. ACM Spec. Interest Group Data Commun.* https://doi.org/10.1145/3230543.3230566 (ACM, 2018).
200. Park, S. et al. Self-powered ultra-flexible electronics via nano-grating-patterned organic photovoltaics. *Nature* **561**, 516–521 (2018).
201. Meng, B. et al. A transparent single-friction-surface triboelectric generator and self-powered touch sensor. *Energy Environ. Sci.* **6**, 3235–3240 (2013).
202. Nan, K. et al. Compliant and stretchable thermoelectric coils for energy harvesting in miniature flexible devices. *Sci. Adv.* **4**, eaau5849 (2018).
203. Song, Y. et al. Wireless battery-free wearable sweat sensor powered by human motion. *Sci. Adv.* **6**, eaay9842 (2020).
204. Yu, Y. et al. Biofuel-powered soft electronic skin with multiplexed and wireless sensing for human-machine interfaces. *Sci. Robot* **5**, eaaz7946 (2020).
205. Yao, G. et al. Effective weight control via an implanted self-powered vagus nerve stimulation device. *Nat. Commun.* **9**, 5349 (2018).
206. Dagdeviren, C. et al. Conformal piezoelectric energy harvesting and storage from motions of the heart, lung, and diaphragm. *Proc. Natl Acad. Sci. USA* **111**, 1927–1932 (2014).
207. Yang, S.-Y. et al. Powering implantable and ingestible electronics. *Adv. Funct. Mater.* **31**, 2009289 (2021).
A review of the challenges and advances in powering long-term in vivo electronics.
208. Nan, K. et al. Low-cost gastrointestinal manometry via silicone–liquid-metal pressure transducers resembling a quipu. *Nat. Biomed. Eng.* https://doi.org/10.1038/s41551-022-00859-5 (2022).
209. Adams, J. B., Johansen, L. J., Powell, L. D., Quig, D. & Rubin, R. A. Gastrointestinal flora and gastrointestinal status in children with autism–comparisons to typical children and correlation with autism severity. *BMC Gastroenterol.* **11**, 22 (2011).
210. Han, B. Correlation between gastrointestinal hormones and anxiety-depressive states in irritable bowel syndrome. *Exp. Ther. Med.* **6**, 715–720 (2013).
211. Hill, J. M., Bhattacharjee, S., Pogue, A. I. & Lukiw, W. J. The gastrointestinal tract microbiome and potential link to Alzheimer's disease. *Front. Neurol.* **5**, 43 (2014).
212. Chu, J. N. & Traverso, G. Foundations of gastrointestinal-based drug delivery and future developments. *Nat. Rev. Gastroenterol. Hepatol.* **19**, 219–238 (2022).
A review of the materials and devices that can interface with the GI mucosa for long-term and sustained drug delivery.
213. Zhao, Z., Ukidve, A., Kim, J. & Mitragotri, S. Targeting strategies for tissue-specific drug delivery. *Cell* **181**, 151–167 (2020).
214. Siegel, R. A. & Rathbone, M. J. in *Fundamentals and Applications of Controlled Release Drug Delivery* (eds Siepmann, J., Siegel, R. & Rathbone, M.) 19–43 (Springer, 2012).
215. Yan, J., Lu, Y., Chen, G., Yang, M. & Gu, Z. Advances in liquid metals for biomedical applications. *Chem. Soc. Rev.* **47**, 2518–2533 (2018).
216. Asplund, M. et al. Toxicity evaluation of PEDOT/biomolecular composites intended for neural communication electrodes. *Biomed. Mater.* **4**, 045009 (2009).
217. Jiang, Y. et al. Topological supramolecular network enabled high-conductivity, stretchable organic bioelectronics. *Science* **375**, 1411–1417 (2022).
218. International Organization for Standardization (ISO). *Biological Evaluation of Medical Devices — Part 1: Evaluation and testing within a risk management process*. ISO 10993-1:2018 (2018).
219. Bass, D. M., Mary, P. & Waxman, D. S. Gastrointestinal safety of an extended-release, nondeformable, oral dosage form (OROS): A retrospective study. *Drug Saf.* **25**, 1021–1033 (2002).

220. Li, J., Liang, J. Y., Laken, S. J., Langer, R. & Traverso, G. Clinical opportunities for continuous biosensing and closed-loop therapies. *Trends Chem.* **2**, 319–340 (2020).
This review establishes several clinical opportunities for continuous biosensing, particularly when coupled with drug delivery strategies to enable closed-loop therapies.
221. Gulshan, V. et al. Development and validation of a deep learning algorithm for detection of diabetic retinopathy in retinal fundus photographs. *JAMA* **316**, 2402–2410 (2016).
222. Shashikumar, S. P., Shah, A. J., Li, Q., Clifford, G. D. & Nemati, S. in *Proc. 2017 IEEE EMBS Int. Conf. Biomed. Health Inform.* https://doi.org/10.1109/bhi.2017.7897225 (IEEE, 2017).
223. Manogaran, G. et al. Wearable IoT smart-log patch: An edge computing-based Bayesian deep learning network system for multi access physical monitoring system. *Sensors* **19**, 3030 (2019).
224. Torres-Soto, J. & Ashley, E. A. Multi-task deep learning for cardiac rhythm detection in wearable devices. *NPJ Digit. Med.* **3**, 116 (2020).
225. Kim, D.-H. et al. Epidermal electronics. *Science* **333**, 838–843 (2011).
This study is one of the first demonstrations of 'epidermal electronics', a set of physiological sensors that mechanically resemble the epidermis and can facilitate seamless device integration with the mucosa.
226. Li, Q. et al. Cyborg organoids: implantation of nanoelectronics via organogenesis for tissue-wide electrophysiology. *Nano Lett.* **19**, 5781–5789 (2019).
227. Choi, Y. S. et al. Fully implantable and bioresorbable cardiac pacemakers without leads or batteries. *Nat. Biotechnol.* **39**, 1228–1238 (2021).
One of the first demonstrations of a fully bioresorbable, wireless cardiac pacemaker fitted in living rodents, which has implications for designing bioresorbable MIE that can avoid surgical removal.
228. Miyamoto, A. et al. Inflammation-free, gas-permeable, lightweight, stretchable on-skin electronics with nanomeshes. *Nat. Nanotechnol.* **12**, 907–913 (2017).
229. Lee, S. et al. Ultrasoft electronics to monitor dynamically pulsing cardiomyocytes. *Nat. Nanotechnol.* **14**, 156–160 (2019).
230. Liu, J. et al. Intrinsically stretchable electrode array enabled in vivo electrophysiological mapping of atrial fibrillation at cellular resolution. *Proc. Natl Acad. Sci. USA* **117**, 14769–14778 (2020).
231. Minev, I. R. et al. Electronic dura mater for long-term multimodal neural interfaces. *Science* **347**, 159–163 (2015).
232. Koster, M. I. Making an epidermis. *Ann. N. Y. Acad. Sci.* **1170**, 7–10 (2009).
233. Williams, J. M. et al. Epithelial cell shedding and barrier function. *Vet. Pathol.* **52**, 445–455 (2015).
234. Balsara, Z. R. & Li, X. Sleeping beauty: awakening urothelium from its slumber. *Am. J. Physiol. Renal Physiol.* **312**, F732–F743 (2017).
235. Deshmukh, S. & Nayak, S. in *Hysteroscopy Simplified by Masters* (eds Tandulwadkar, S. & Pal, B.) 53–62 (Springer, 2021).
236. Rao, J. N. & Wang, J.-Y. in *Regulation of Gastrointestinal Mucosal Growth* (Morgan & Claypool Life Sciences, 2010).
237. Fry, C. H. & Vahabi, B. The role of the mucosa in normal and abnormal bladder function. *Basic Clin. Pharmacol. Toxicol.* **119**, 57–62 (2016).
238. Munkholm, M. & Mortensen, J. Mucociliary clearance: pathophysiological aspects. *Clin. Physiol. Funct. Imaging* **34**, 171–177 (2014).
239. Linden, S. K., Sutton, P., Karlsson, N. G., Korolik, V. & McGuckin, M. A. Mucins in the mucosal barrier to infection. *Mucosal Immunol.* **1**, 183–197 (2008).
240. Thiyagarajan, D. K., Basit, H. & Jeanmonod, R. Physiology, menstrual cycle. *StatPearls* [online] https://www.ncbi.nlm.nih.gov/books/NBK500020/ (updated 30 Oct 2021).
241. Boegh, M. & Nielsen, H. M. Mucus as a barrier to drug delivery–understanding and mimicking the barrier properties. *Basic Clin. Pharmacol. Toxicol.* **116**, 179–186 (2015).
242. Zhu, C., Chen, Z. & Jiang, Z. Expression, distribution and role of aquaporin water channels in human and animal stomach and intestines. *Int. J. Mol. Sci.* **17**, 1399 (2016).
243. Dave, L. A., Montoya, C. A., Rutherfurd, S. M. & Moughan, P. J. Gastrointestinal endogenous proteins as a source of bioactive peptides - an in silico study. *PLoS ONE* **9**, e98922 (2014).
244. Rouprêt, M. et al. Can ureteral stent encrustation analysis predict urinary stone composition? *Urology* **66**, 246–251 (2005).
245. Lim, C. L., Byrne, C. & Lee, J. K. Human thermoregulation and measurement of body temperature in exercise and clinical settings. *Ann. Acad. Med. Singap.* **37**, 347–353 (2008).
246. Kalantar-Zadeh, K., Berean, K. J., Burgell, R. E., Muir, J. G. & Gibson, P. R. Intestinal gases: influence on gut disorders and the role of dietary manipulations. *Nat. Rev. Gastroenterol. Hepatol.* **16**, 733–747 (2019).
247. Yang, W. H. & Shen, N. C. Gas-forming infection of the urinary tract: an investigation of fermentation as a mechanism. *J. Urol.* **143**, 960–964 (1990).
248. Němeček, D., Dvořáková, M. & Sedmíková, M. Heme oxygenase/carbon monoxide in the female reproductive system: an overlooked signalling pathway. *Int. J. Biochem. Mol. Biol.* **8**, 1–12 (2017).
249. Anahtar, M. N., Gootenberg, D. B., Mitchell, C. M. & Kwon, D. S. Cervicovaginal microbiota and reproductive health: the virtue of simplicity. *Cell Host Microbe* **23**, 159–168 (2018).
250. Hillman, E. T., Lu, H., Yao, T. & Nakatsu, C. H. Microbial ecology along the gastrointestinal tract. *Microbes Environ.* **32**, 300–313 (2017).
251. Hooper, L. V. Epithelial cell contributions to intestinal immunity. *Adv. Immunol.* **126**, 129–172 (2015).
252. Huffnagle, G. B., Dickson, R. P. & Lukacs, N. W. The respiratory tract microbiome and lung inflammation: a two-way street. *Mucosal Immunol.* **10**, 299–306 (2017).
253. Delmas, P., Hao, J. & Rodat-Despoix, L. Molecular mechanisms of mechanotransduction in mammalian sensory neurons. *Nat. Rev. Neurosci.* **12**, 139–153 (2011).
254. Sengupta, J. N. An overview of esophageal sensory receptors. *Am. J. Med.* **108**, 87S–89S (2000).
255. Dalesio, N. M., Barreto Ortiz, S. F., Pluznick, J. L. & Berkowitz, D. E. Olfactory, taste, and photo sensory receptors in non-sensory organs: it just makes sense. *Front. Physiol.* **9**, 1673 (2018).
256. Jänig, W. *Integrative Action of the Autonomic Nervous System* (Cambridge Univ. Press, 2006).

Acknowledgements
B.Y. acknowledges support from Natural Sciences and Engineering Research Council of Canada's Postdoctoral Fellowships Program (PDF-557493-2021). V.R.F. was supported by the Schmidt Science Fellows programme. G.T. was supported in part by the Karl van Tassel (1925) Career Development Professorship and the Department of Mechanical Engineering, MIT.

Author contributions
All authors researched data for the article. G.T., K.N., V.R.F. and B.Y. contributed substantially to discussion of the content. All authors wrote the article. All authors reviewed and/or edited the manuscript before submission.

Competing interests
Financial competing interests for G.T. that may be interpreted as related to the current manuscript include current and prior funding from Novo Nordisk, Hoffman La Roche, Oracle, Draper Laboratory, MIT Lincoln Laboratory, NIH (NIBIB and NCI), Bill and Melinda Gates Foundation, The Leona M. and Harry B. Helmsley Charitable Trust, Karl van Tassel (1925) Career Development Professor, MIT and the Defense Advanced Research Projects Agency, as well as employment by the Massachusetts Institute of Technology and Brigham and Women's Hospital. Personal financial interests include equity/stock (Lyndra Therapeutics, Suono Bio, Vivtex, Celero Systems, Syntis Bio), board of directors member and/or consultant (Lyndra Therapeutics, Novo Nordisk, Suono Bio, Vivtex, Celero Systems, Syntis Bio) and royalties (past and potentially in the future) from licensed and/or optioned intellectual property (Lyndra Therapeutics, Novo Nordisk, Suono Bio, Vivtex, Celero Systems, Syntis Bio, Johns Hopkins, MIT, Mass General Brigham Innovation). Complete details of all relationships for profit and not-for-profit for G.T. can be found in the supplementary information. K.N. and G.T. report a patent application (U.S. Provisional Application no. 63/301,491) describing a flexible silicone liquid-metal-filled manometry system. G.T. reports the following patents and/or patent applications: U.S. patent no. 10,149,635 describing ingestible devices for physiological status monitoring, U.S. patent nos. 10,182,985, 10,413,507, 10,517,819, 10,517,820, 10,532,027, 10,596,110, 10,610,482, 10,716,751 and 10,716,752 describing gastric residence structures and materials supporting safe residence and GI transit, U.S. patent nos. 10,693,544 and 10,879,983 describing methods for charging of GI devices through RF transmission, U.S. patent no. 11,207,272 describing a device with gastric anchoring capabilities and the capacity for electrical stimulation and sensing, U.S. Provisional Application patent no. 16/152,785 describing a flexible piezoelectric device that can sense deformation in the GI tract, U.S. Provisional Application patent no. 16/207,647 a gastric resident electronic device, U.S. Provisional Application patent no. 17/470,942 describing a gastric resident system capable of sensing radiation and toxic agents and releasing therapeutics, U.S. Provisional Application patent no. 63/246,761 describing a nasogastric system for biochemical sensing and U.S. Provisional Application patent no. 63/294,902 describing a system for energy harvesting from the GI tract. All other authors declare no competing interests.

Peer review information
Nature Reviews Materials thanks Changhyun Pang and the other, anonymous, reviewer(s) for their contribution to the peer review of this work.

Publisher's note
Springer Nature remains neutral with regard to jurisdictional claims in published maps and institutional affiliations.

Springer Nature or its licensor holds exclusive rights to this article under a publishing agreement with the author(s) or other rightsholder(s); author self-archiving of the accepted manuscript version of this article is solely governed by the terms of such publishing agreement and applicable law.

Supplementary information
The online version contains supplementary material available at https://doi.org/10.1038/s41578-022-00477-2.

© Springer Nature Limited 2022